JCB

The GTPase activating protein Gyp7 regulates Rab7/Ypt7 activity on late endosomes

Nadia Füllbrunn, Raffaele Nicastro, Muriel Mari, Janice Griffith, Eric Herrmann, Rene Rasche, Ann-Christin Borchers, Kathrin Auffarth, Daniel Kümmel, Fulvio Reggiori, Claudio De Virgilio, Lars Langemeyer, and Christian Ungermann

Corresponding Author(s): Christian Ungermann, Osnabrück University

Review Timeline:

Submission Date:	2023-05-12
Editorial Decision:	2023-07-13
Revision Received:	2024-01-22
Editorial Decision:	2024-02-27
Revision Received:	2024-03-06

Monitoring Editor: Harald Stenmark

Scientific Editor: Tim Fessenden

Transaction Report:

(Note: With the exception of the correction of typographical or spelling errors that could be a source of ambiguity, letters and reports are not edited. The original formatting of letters and referee reports may not be reflected in this compilation.)

DOI: https://doi.org/10.1083/jcb.202305038

July 13, 2023

Re: JCB manuscript #202305038

Prof. Christian Ungermann
Osnabrück University
Biology/Chemistry
Barbarastrasse 13
Osnabrück 49076
Germany

Dear Prof. Ungermann,

Thank you for submitting your manuscript entitled "The GTPase activating protein Gyp7 regulates the activity of the Rab7-like Ypt7 and signaling at late endosomes". The manuscript has been evaluated by expert reviewers, whose reports are appended below. Unfortunately, after an assessment of the reviewer feedback, our editorial decision is against publication in JCB.

You will see that reviewers commended the intriguing new observations on the regulation of Ypt7 by the GAP Gyp7 based in part on its membrane localization. However, reviewers raised significant concerns over data interpretation and controls, which reduced their confidence in the main conclusions set forth in this study. In particular, Reviewer 2 noted that multiple important conclusions relied on overexpression constructs without confirmation of key results using endogenous gene expression levels. This reviewer also sought evidence of Ypt7 GTPase activity and vacuole lipid composition (point 4). Multiple reviewers also requested measurements of Ypt7 localization at endosomes vs at vacuoles. Last, Reviewer 1 requested improvements to the text towards greater clarity.

We feel that the requests made by the reviewers are more substantial than can be addressed in a typical revision period. If you wish to expedite publication of the current data, it may be best to pursue publication at another journal. However, given interest in the topic and the JCB's interest in publishing this work, we would be open to resubmission to JCB of a significantly revised manuscript that fully addresses the reviewers' concerns noted above and is subject to further peer-review. Should you wish to pursue publication with a revised manuscript, please provide a plan for revision in an appeal request. Please note that we may discuss the revision plan with at least one reviewer. If and when you would like to resubmit this work to JCB, please contact the journal office to discuss an appeal of this decision or you may submit an appeal directly through our manuscript submission system.

Regardless of how you choose to proceed, we hope that the comments below will prove constructive as your work progresses. We would be happy to discuss the reviewer comments further once you've had a chance to consider the points raised in this letter. You can contact the journal office with any questions, cellbio@rockefeller.edu or call (212) 327-8588.

Thank you for thinking of JCB as an appropriate place to publish your work.

Sincerely,

Harald Stenmark
Monitoring Editor
Journal of Cell Biology

Tim Fessenden
Scientific Editor
Journal of Cell Biology

Reviewer #1 (Comments to the Authors (Required)):

This is an interesting study investigating the function of the Rab-GAP Gyp7 in budding yeast. The authors use a combination of approaches to characterize the role of Gyp7 in regulation of Ypt7, the yeast Rab7 homolog.

The authors show that Gyp7 localizes to endosomes and that forcing Gyp7 to localize to the vacuole (yeast lysosome) by fusing

it to vacuolar proteins alters vacuolar morphology. They also find that Gyp7 is required for normal cellular resistance to ZnCl2 and rapamycin and efficient endocytosis of Mup1, indicating loss of Gyp7 sensitizes cells to endocytic stress and TORC1 inhibition.

The authors find that Gyp7 localization does not require several endosomal proteins for its localization. In order to gain more information regarding how Gyp7 localizes to endosomes, the authors perform in vitro studies in which they examine the requirements for Gyp7 membrane-binding and GAP activity. They find that Gyp7 binds well to and has Ypt7 GAP activity upon liposomes comprised of vacuolar lipids but not simple PC/PE lipids. Interestingly, even when Gyp7 is forced to bind to PC/PE liposomes, using a His-tag and nickel-chelated-lipids, Gyp7 but is still not very active. This suggests a specific membrane environment is important for both binding and activity of Gyp7.

They find that while loss of Gyp7 has no obvious effect on Ypt7 localization, overexpression of Gyp7 essentially removes Ypt7 from the lysosome (vacuole) membrane and therefore results in enrichment of Ypt7 on endosomes. They find that hyperactivation of Ypt7 at endosomes by overexpression of Gyp7 slows the kinetics of Mup1 endocytosis. Interestingly, this means that both loss of Gyp7 and overexpression of Gyp7 have similar effects on endocytosis. They also find that hyperactivation of Ypt7 on endosomes results in slight resistance to rapamycin. Finally, they observe that overexpression of Gyp7 results in accumulation of the endocytic tracer FM-464 in Ypt7-positive endosomes in the absence of ESCRT function. Taken together the authors interpret these results to mean that Ypt7 functions on "signaling" endosomes.

Overall this is an interesting study but at times I found the explanation or interpretation of results to be a bit unclear. Below are my suggestions for improvement:

1. I found the presentation of the Gyp7 localization results to be a bit unclear regarding which compartment the authors consider it to localize to. Is it possible that the differential localization of Gyp7 and other endosomal proteins reflects different timing/kinetics rather than distinct compartments? For example, different Golgi proteins appear to have different localizations but when observed over time they are seen to localize to the same compartment just with different kinetics. This possibility is mentioned in the discussion but it would be good to clarify and mention this possibility when the results are presented. These are the phrases that made me a bit confused: "We further show that Gyp7 overproduction can retain Ypt7 on late endosomes, which enhances endosomal TORC1 signaling. These Ypt7-positive endosomes lack ESCRTs, yet require ESCRTs for their formation. We thus speculate that these late endosomes correspond to signaling endosomes." and "We thus conclude that Ypt7 functions on mature MVBs, which in part correspond to signaling endosomes." Are signaling endosomes a subset of late endosomes? How are they defined?

2. Similarly, can the authors include at an earlier point in their manuscript an explicit description of how they are distinguishing "signaling endosomes" from "late endosomes", and also how each of these relates to what has been called the "pre-vacuolar endosome (PVE)"? They have some description of signaling endosomes in the discussion, but I found it confusing to see this term mentioned multiple times in the results sections without understanding how they are distinguishing a signaling endosome from a late endosome or PVE.

3. In Figure 1, how can the authors distinguish the difference between disrupted endosomal morphology versus disrupted Gyp7 recruitment to endosomes? Also, what is special about Mvp1 versus other ESCRT components?

4. The following two statements seem to conflict with each other, and I think the second statement is more accurate than the first statement:
"Our data suggest that a functional Rab5 system is required for correct Gyp7 localization to endosomes." (line 165)
"This suggests that Gyp7 recruitment to endosomes occurs independent of the analyzed endosomal proteins. (line 176)

5. It would be very helpful to include a more straightforward analysis of the relationship between Gyp7 and Ypt7 localizations. The experiments involving how overexpression of Gyp7 induce more Ypt7 localization at endosomes, which is apparently the same compartment where Gyp7 itself localizes, are a bit puzzling. In principle one would expect a GAP to antagonize the localization of its Rab. One possibility is that overexpression of Gyp7 causes a shift in localization of Gyp7 to the vacuole. It would be straightforward for the authors to test if this is the case by repeating the Gyp7 overexpression experiments using a fluorescent-tagged version of Gyp7. This could potentially provide a simple explanation for the observed effects on Ypt7 localization. For example, in Figure 6A, the localization of Ypt7 is shown with and without Gyp7 and when Gyp7 is overexpressed, but Gyp7 localization itself is not observed at the same time. Do Gyp7 and Ypt7 normally co-localize? Do they colocalize when Gyp7 is overexpressed?

6. I think the sentence: "Thus, Gyp7 function is required for normal TORC1 activity within the endolysosomal system" (lines 220-221) is a bit of an overstatement at this point in the manuscript because the authors have only shown sensitivity to Rapamycin and have not shown any direct measure of TORC1 activity (i.e. changes in substrate phosphorylation).

7. The loss of Gyp7 function does not affect Ypt7 localization. One might expect Ypt7 to have a more broad or intense localization in the absence of its GEF. Can the authors comment on whether this might be because another GYP gene also acts

as a GAP for Ypt7?

8. There appears to be some redundancy in these two sentences: (line 406) "Surprisingly, Gyp7 overproduction does not liberate Ypt7 from endosomes, but rather confines it to a subpopulation proximal to the vacuole. This effect is even stronger when Gyp7 is overexpressed, and ..."

Reviewer #2 (Comments to the Authors (Required)):

In this clearly written manuscript, Füllrunn and coworders report studies of the budding yeast Rab GAP Gyp7. They present genetic and cell biological studies which confirm and extend prior work from three other labs showing that Gyp7 is the major GAP that inactivates Rab7 (Ypt7), and present data which they interpret to indicate that an endosomal compartment or compartments is the major in vivo site of Gyp7 action. Biochemical experiments show that Gyp7 has a membrane binding activity that exhibits selectivity for lipid composition. Several of the reported experiments are interesting but as discussed below key conclusions are based on non-physiological genetic perturbations (overexpression) and several experiments do not include controls necessary for interpretation of the results, tempering my enthusiasm for the manuscript. It is possible that some of the needed data are already in hand but not shown. With some additions and a more tempered interpretation of the results, I'd be happy to take another look at this study.

Major points.

1. "Gyp7 localizes to endosomes." [line 142] The authors show that overexpressed Gyp7 localizes to punctate structures that appear to label with the endocytic tracer FM4-64. However, no co-localization with known protein markers of endosomes is shown, except to a limited extent in a vps4Δ background, where dozens of markers accumulate at class E compartments. This is an odd omission. Moreover, the authors see *more* localization of Gyp7 to punctate structures when Rab5 or Rab5 effector function is impaired, not less - and these punctae do not seem to be marked by FM4-64. It is hard to see this as support for the hypothesis that Gyp7 localizes to endosomes. Could these be, for example, Atg8 accumulations rather than endosomes?

2. "Relocalization of Gyp7 to vacuoles impairs vacuole morphology." [line 178] This is a reasonable conclusion on the basis of overexpresison as previously reported and experiments shown here (Fig. 2A,B). However, the re-targeting experiments (Fig. 2C,E) show much larger effects for the affinity-tagged Vac8-CB used as an anchor to relocalize Gyp7 than for the relocalization itself. Or perhaps I'm misreading the experiment? I asked two other experienced people in my lab to read this section of the paper, and they read it the same way. I don't see how this experiment can be interpreted using a background with what seems to be a reasonably strong vac8 hypomorph.

Additionally, it's hard to see how expression of a presumptively spontaneous nucleotide-exchanging variant of Ypt7 is a better control here than a catalytic-dead Gyp7 (R458K), as used in previous studies (Eitzen, EMBO J 2000; Brett, JCB 2008). Use of this well-characterized mutant could have strengthened several experiments in the present study. It's perplexing that R458K was not employed in this study.

3. (Gyp7 is required for homeostasis of the endosomal system."[line 204] The authors show data suggesting that perturbation of Gyp7 function alters TORC1 signaling, consistent with the known role of endolysososmal traffic in the TORC1 pathway. It is interesting that an msb3 (Rab5 GAP) mutant phenocopies the gyp7 deletion for this readout.

Data are also shown suggesting that traffic kinetics through the endosomal MVB pathway to the vacuole are (very) subtly regulated by Gyp7 activity. The experiments do not clearly delineate whether the target of this regulation is Ypt7 residing on the endosome, on the vacuole, or both.

4. "Gyp7 activity depends on the membrane environment." [line 232]. It is persuasively shown that Gyp7 binds membranes, that it prefers to bind membranes with a vacuole-like membrane mixture (an endosomal vs. vacuole lipid mixture was not tested, as might have been expected given the overall argument of the paper), and that this activity depends on a PH-like domain near the protein's N-terminus. The PH-like domain alone does not bind membranes in the experimental configurations employed.

The authors use mainly GDI extraction as a proxy for Gyp7 activity against Ypt7/Rab7. There's nothing wrong with this approach, as such. But curiously direct assay of Ypt7 GTPase activity is reported solely in Fig. 5J. The authors claim that this shows allosteric regulation of Gyp7 activity against soluble (non-lipidated) Ypt7 by membranes. The result shows a very small but apparently reproducible difference in activity. But given the advantages of a chemically defined system, why was GTPase activity not assayed directly throughout? This is not hard to do using well-described colorimetric, fluorescence, or [32]P orthophosphate release assays, or presumably the HPLC assay in Fig. 5J.

Given the absence of direct readouts of GTP hydrolysis, it is important to test whether the lipid mix used (VML vs. PC/PE) influences the ability of GDI to extract Ypt7-GDP. This control is important if extraction is used as the main proxy for the Rab's

nucleotide state. Also, it was not clear to this reader whether GDI is present in excess to Ypt7, or what the final GDI concentration was in the extraction experiments.

Overall, the experiments support the idea that direct membrane association increases Gyp7 activity against Ypt7. They do not strongly support the idea that membrane association has a major allosteric effect on Gyp7 catalytic activity.

5. "Gyp7 activity confines Ypt7 to late endosomes and signaling endosomes." Taken literally, this is obviously wrong, since Ypt7 on vacuoles is needed for vacuole fusion, as exhaustively demonstrated by many labs including the authors', and the data show (as entirely expected) lots of Ypt7 on the vacuole in wild type cells. Fig. 6A also shows that overproduction of Gyp7 removes Ypt7 from the vacuole, and if anything, increases its localization to (presumptively) endosomal punctae. This would seem to argue that Gyp7 preferentially targets Ypt7 on the vacuole, not on the endosome as the authors suggest earlier in the manuscript.

Other experiments here are based on a truncation of the GEF subunit Mon1 that results in elevated Ypt7 activity, as nicely shown in recent work from the same group. But Gyp7 is not shown to colocalize with Mon1 or Ypt7 under these circumstances. An interesting observation is that endosomes marked by Pep12 increase in number in a MON1Δ100 mutant that also overproduces Gyp7. However, it's not tested whether this phenotype is due to one of these genetic manipulations, or both (Fig. 6E).

6. "Endolysosomal transport is delayed upon Ypt7 confinement to late endosomes." [line 338]. The delays are again subtle but apparently statistically significant, and consistent with the ability of Gyp7 to deplete Ypt7 from the vacuole as shown in Fig. 6A.

7. "Ypt7-positive structures correspond to signaling endosomes." Immunogold EM shows that overproduced Ypt7 can be detected on endosomal structures, and Ypt7 accumulates on Class E compartments in a vps4Δ mutant (along with dozens of other endolysosomal proteins). In Fig. S6A,B a reporter system is used to assay endosomal vs. vacuolar phosphorylation of Sch9 by Tor1. In a gyp7Δ mutant vs. wild type, a significant decrease in TORC1 activity is seen at the vacuole and *not* at the endosome. Overproduction does increase signaling at the endosome, but given the lack of a deletion phenotype, this is not a strong argument for a normal physiological function of Gyp7 at the endosome per se. I wonder if stronger phenotypes would emerge in nitrogen limited conditions.

Minor issues.

8. The paper by Eitzen (EMBO J 2000) is not cited, and should be.
9. Line 216: In yeast, Apl5 is not an endosomal trafficking protein.
10. Line 224: Fig. 3C is not mentioned in the Results, so far as I can tell.
11. Fig. S2B: genotypes should be labeled.

- Alexey Merz

Reviewer #3 (Comments to the Authors (Required)):

In the present study, Füllbrunn et al. dissect the endocytic localization and function of the Ypt7 (RAB7) specific GAP protein Gyp7 in yeast. While Gyp7 is already known to be a GAP for RAB7, the precise localization and membrane dependency of Ypt7 inactivation through Gyp7 remained to be elucidated.

The authors demonstrate that Gyp7 localizes primarily to endosomes but not to the vacuole and that this localization partially depends on an intact Vps21 (RAB5) system. Additional localization experiments indicate that Gyp7 functions on endosomes but likely not on the vacuolar membrane. Deletion of Gyp7 delayed endosomal transport towards the vacuole and altered endosomal mTORC1 signaling, suggesting that Gyp7 is required for the homeostasis and signaling function of endosomes. In an additional line of experimentation, the authors demonstrate that Gyp7 requires endosomal membranes for its GAP activity as membrane free Gyp7 was hardly active towards Ypt7. Finally, the authors demonstrate that Gyp7 activity confines Ypt7 to late endosomes which are also signaling endosomes.

Overall, the data is of high quality and the authors' conclusions appear reasonable to this reviewer. The authors thoroughly dissect the localization of Gyp7, its effect on Ypt7 and its role within the endocytic network. With this being said, I think that the manuscript is somewhat uninspiring as Gyp7 was already known to be the dominant Ypt7 GAP protein in yeast . It is still a solid and thorough cell biological analysis of a previously known RAB7 GAP in yeast but it doesn't add a lot of groundbreaking insight into the function of this endocytic protein. While I am generally supportive of publication I am not sure whether JCB is an appropriate venue for this manuscript.

Minor points:

Figure 4A: "floatation" seems odd

Response to the reviewers (Füllbrunn et al., CB manuscript #202305038)

Below is a list of experiments that we performed to address the reviewers' comments:

- Determine the precise localization of Gyp7 in the endosomal system:
  - Localization of Gyp7 relative to endosomal and other organellar marker proteins (Vps8, Vps21, Ccz1, Vps35, Vps5, Vps4, Ivy1, Mnn9, Sec7, Ypt7) (Reviewer #1 and #2, not incorporated in Figures, attached to this document)
  - Localization of fluorescently-labeled Gyp7 relative to endogenously expressed Ypt7 and Mon1-Ccz1 in wild-type vs. Gyp7-overproducing vs. Mon1Δ100-Ccz1 expressing cells (Reviewer #1 and #2; Figure 6C-E)

- Determine if another GAP can replace Gyp7:
  - Localization of Ypt7 in *gyp7*Δ *msb3*Δ cells (Reviewer #1, Figure S5A-B)

- Show that Gyp7 activity is responsible for the vacuole phenotype due to relocalization:
  - Relocalization of wild-type Gyp7 and the catalytic-deficient Gyp7 mutant (R458K) to vacuoles with a Chromobody attached to the vacuolar protein Zrc1 (Reviewer #2; Figure 2C-G)

- Establish whether GDI extracts Ypt7 on all membranes:
  - Gyp7 activity towards Ypt7 on VMLs vs. PC/PE liposomes in the presence of excess GDI (Reviewer #2, Figure S3A-B)
  - GDI extraction assay: Gyp1-46 activity towards Ypt7 on VMLs vs. PC/PE liposomes (Reviewer #2, Figure 4L-M)

- Determine which of the two factors (hyperactive GEF, Mon1$^{\Delta 100}$, or Gyp7 overproduction) has the predominant effect on the endosomal system:
  - Localization of Pep12 in Mon1$^{\Delta 100}$-Ccz1 expressing vs. Gyp7-overproducing cells (Reviewer #2, Figure 7C-D, S6B)

- Examine whether the *gyp7*Δ mutant has a stronger phenotype if challenged by nitrogen starvation, we analyzed the vacuole morphology under these conditions (Reviewer #2, Figure 3G-H)

- Furthermore, we implemented electron microscopy analysis of cells expressing mNeon-Ypt7 in wild-type and Mon1$^{\Delta 100}$-Ccz1 *TEF1*pr-*GYP7* cells to analyze a potential effect on MVBs (morphology and number per cell) (Figure 9C).

Reviewer #1 (Comments to the Authors (Required)):

This is an interesting study investigating the function of the Rab-GAP Gyp7 in budding yeast. The authors use a combination of approaches to characterize the role of Gyp7 in regulation of Ypt7, the yeast Rab7 homolog.

The authors show that Gyp7 localizes to endosomes and that forcing Gyp7 to localize to the

vacuole (yeast lysosome) by fusing it to vacuolar proteins alters vacuolar morphology. They also find that Gyp7 is required for normal cellular resistance to ZnCl2 and rapamycin and efficient endocytosis of Mup1, indicating loss of Gyp7 sensitizes cells to endocytic stress and TORC1 inhibition.

The authors find that Gyp7 localization does not require several endosomal proteins for its localization. In order to gain more information regarding how Gyp7 localizes to endosomes, the authors perform in vitro studies in which they examine the requirements for Gyp7 membrane-binding and GAP activity. They find that Gyp7 binds well to and has Ypt7 GAP activity upon liposomes comprised of vacuolar lipids but not simple PC/PE lipids. Interestingly, even when Gyp7 is forced to bind to PC/PE liposomes, using a His-tag and nickel-chelated-lipids, Gyp7 but is still not very active. This suggests a specific membrane environment is important for both binding and activity of Gyp7.

They find that while loss of Gyp7 has no obvious effect on Ypt7 localization, overexpression of Gyp7 essentially removes Ypt7 from the lysosome (vacuole) membrane and therefore results in enrichment of Ypt7 on endosomes. They find that hyperactivation of Ypt7 at endosomes by overexpression of Gyp7 slows the kinetics of Mup1 endocytosis. Interestingly, this means that both loss of Gyp7 and overexpression of Gyp7 have similar effects on endocytosis. They also find that hyperactivation of Ypt7 on endosomes results in slight resistance to rapamycin. Finally, they observe that overexpression of Gyp7 results in accumulation of the endocytic tracer FM-464 in Ypt7-positive endosomes in the absence of ESCRT function. Taken together the authors interpret these results to mean that Ypt7 functions on "signaling" endosomes.

Just for clarification - the reviewer might have misunderstood our data in part. If Gyp7 is overproduced, we observe faster endocytosis, whereas the deletion of Gyp7 results in slower endocytosis of Mup1 (Fig. 8D,E).

Overall this is an interesting study but at times I found the explanation or interpretation of results to be a bit unclear. Below are my suggestions for improvement:

1. I found the presentation of the Gyp7 localization results to be a bit unclear regarding which compartment the authors consider it to localize to. Is it possible that the differential localization of Gyp7 and other endosomal proteins reflects different timing/kinetics rather than distinct compartments? For example, different Golgi proteins appear to have different localizations but when observed over time they are seen to localize to the same compartment just with different kinetics. This possibility is mentioned in the discussion but it would be good to clarify and mention this possibility when the results are presented. These are the phrases that made me a bit confused: "We further show that Gyp7 overproduction can retain Ypt7 on late endosomes, which enhances endosomal TORC1 signaling. These Ypt7-positive endosomes lack ESCRTs, yet require ESCRTs for their formation. We thus speculate that these late endosomes correspond to signaling endosomes." and "We thus conclude that Ypt7 functions on mature MVBs, which in part correspond to signaling endosomes." Are signaling endosomes a subset of late endosomes? How are they defined?

We agree with the reviewer that Gyp7 and other endosomal proteins could localize to the same compartment but have different timing/kinetics. Our strongest argument of the endosomal localization is the observation that Gyp7 accumulates in the class E compartment of *vps4*Δ cells. However, we rephrased our statement as we did not really observe a strong colocalization of Gyp7 with any distinct endosomal marker, suggesting a very dynamic association. We did not include this analysis in the data set as not informative, but present it below for the reviewers' information (see also point 1 of Reviewer #2). As we do not know the binding partner of Gyp7, a more specific analysis has to wait the identification of this binding partner.

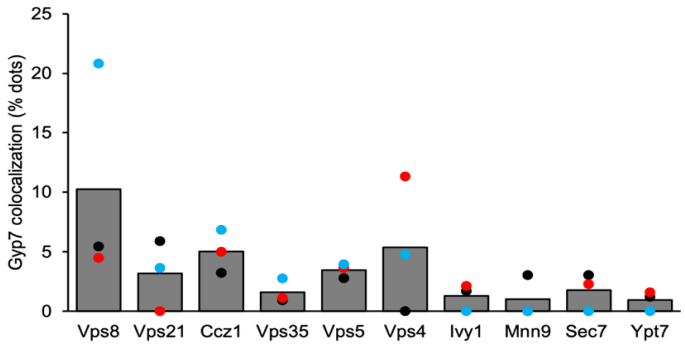

Furthermore, we interpret our results that signaling endosomes are a subset of late endosomes, where Ypt7 resides. In agreement with this, we find that the Ypt7 confinement by Gyp7 overproduction results in the increased resistance of cells to rapamycin, whereas the deletion of *GYP7* causes a hypersensitivity to rapamycin.

2. Similarly, can the authors include at an earlier point in their manuscript an explicit description of how they are distinguishing "signaling endosomes" from "late endosomes", and also how each of these relates to what has been called the "pre-vacuolar endosome (PVE)"? They have some description of signaling endosomes in the discussion, but I found it confusing to see this term mentioned multiple times in the results sections without understanding how they are distinguishing a signaling endosome from a late endosome or PVE.

We agree with the reviewer that the term signaling endosome has to be introduced by taking the previous nomenclature into account. The PVE is probably a mixture of the Vps21-positive endosomes and the Ypt7-positive late endosomes. Within the latter ones, the signaling endosomes will be a subpopulation. We adjusted the introduction accordingly.

3. In Figure 1, how can the authors distinguish the difference between disrupted endosomal morphology versus disrupted Gyp7 recruitment to endosomes? Also, what is special about Mvp1 versus other ESCRT components?

We agree with the reviewer that altered Gyp7 localization in strains lacking endosomal proteins, in particular the Class D mutants (*vps21*Δ *ypt52*Δ, *vps9*Δ *muk1*Δ, *vps3*Δ, *vps45*Δ), could be caused by disrupted endosomal morphology or disrupted recruitment of Gyp7 onto endosomes. Therefore, we now propose two possible scenarios in the text.

Mvp1 is one of the proteins involved in retrograde transport, but is not an ESCRT protein. It is part of a family of proteins with BAR domains (Chi et al., JCS 2014). Interestingly, the

number of Gyp7 puncta per cell is decreased in the *mvp1*Δ deletion mutant but not in other deletion mutants impaired in retrograde transport such as *vps35*Δ, *vps5*Δ, and *snx4*Δ cells (Figure 1E,F, S1A). This suggests that Gyp7 localization is somehow linked to one of the retrograde pathways from the endosome to the Golgi (Suzuki et al., elife 2021).

4. The following two statements seem to conflict with each other, and I think the second statement is more accurate than the first statement:
"Our data suggest that a functional Rab5 system is required for correct Gyp7 localization to endosomes." (line 165)
"This suggests that Gyp7 recruitment to endosomes occurs independent of the analyzed endosomal proteins. (line 176)

We agree with the reviewer that the two statements conflict each other. Gyp7 recruitment does not depend on the presence of single endosomal proteins as their absence does not lead to loss of membrane localization of Gyp7. The differential localization of Gyp7 in all Class D mutants is presumably caused by a disrupted endolysosomal system per se. We adjusted the text accordingly.

5. It would be very helpful to include a more straightforward analysis of the relationship between Gyp7 and Ypt7 localizations. The experiments involving how overexpression of Gyp7 induce more Ypt7 localization at endosomes, which is apparently the same compartment where Gyp7 itself localizes, are a bit puzzling. In principle one would expect a GAP to antagonize the localization of its Rab. One possibility is that overexpression of Gyp7 causes a shift in localization of Gyp7 to the vacuole. It would be straightforward for the authors to test if this is the case by repeating the Gyp7 overexpression experiments using a fluorescent-tagged version of Gyp7. This could potentially provide a simple explanation for the observed effects on Ypt7 localization. For example, in Figure 6A, the localization of Ypt7 is shown with and without Gyp7 and when Gyp7 is overexpressed, but Gyp7 localization itself is not observed at the same time.

We appreciate the reviewer's comment and analyzed the localization of fluorescently-tagged Gyp7 relative to Ypt7 upon endogenous or overexpression Gyp7 as well as upon expression of the hyperactive Mon1$^{\Delta 100}$–Ccz1 (Fig. 6C,E). Gyp7 does not colocalize with Ypt7 puncta in both condition, whereas the colocalization of Gyp7 and the GEF subunit Ccz1 strongly increases upon overexpression of Gyp7 (Fig. 6C,D). This suggests that the Ypt7's GEF and GAP can indeed localize to the same endosomal compartment, while Ypt7 shifts from a vacuolar to an endosomal population. Importantly, overexpressed Gyp7 does not localize to and inactivate Ypt7 on the vacuole.

6. I think the sentence: "Thus, Gyp7 function is required for normal TORC1 activity within the endolysosomal system" (lines 220-221) is a bit of an overstatement at this point in the manuscript because the authors have only shown sensitivity to Rapamycin and have not shown any direct measure of TORC1 activity (i.e. changes in substrate phosphorylation).

The reviewer is right. We can only interpret the endosomal or vacuolar TORC1 activity from Fig. S7 on. We discuss the effect of Gyp7 function on TORC1 activity in more detail below.

7. The loss of Gyp7 function does not affect Ypt7 localization. One might expect Ypt7 to

have a more broad or intense localization in the absence of its GEF. Can the authors comment on whether this might be because another GYP gene also acts as a GAP for Ypt7?

We agree with the reviewer that one might expect altered Ypt7 localization in the absence of its GAP Gyp7, which might be overwritten by the function of another GAP. Indeed, our previous study indicated that the GAP of Vps21 and Sec4, Msb3, can inactivate Ypt7 as well, since it inhibits *in vitro* vacuole fusion (Lachmann et al., 2012). Therefore, we analyzed Ypt7 localization in the *msb3*Δ mutant as well as in the *gyp7*Δ *msb3*Δ strain (Fig. S5 A-B). Interestingly, we noticed a slight, though significant decrease in the number of Ypt7 puncta per cell in the double deletion strain, indicating that indeed multiple GAPs could affect Ypt7 localization and activity. However, we believe that Gyp7 is the major Ypt7 GAP as also shown in previous studies and other GAPs probably function only upon loss of Gyp7 function or under certain conditions. This could explain why loss of Gyp7 function alone does not affect Ypt7 localization. We incorporated this possibility in the text accordingly.

8. There appears to be some redundancy in these two sentences: (line 406) "Surprisingly, Gyp7 overproduction does not liberate Ypt7 from endosomes, but rather confines it to a subpopulation proximal to the vacuole. This effect is even stronger when Gyp7 is overexpressed, and ..."

We agree with the reviewer and modified the text accordingly.

Reviewer #2 (Comments to the Authors (Required)):

In this clearly written manuscript, Füllbrunn and coworkers report studies of the budding yeast Rab GAP Gyp7. They present genetic and cell biological studies which confirm and extend prior work from three other labs showing that Gyp7 is the major GAP that inactivates Rab7 (Ypt7), and present data which they interpret to indicate that an endosomal compartment or compartments is the major in vivo site of Gyp7 action. Biochemical experiments show that Gyp7 has a membrane binding activity that exhibits selectivity for lipid composition. Several of the reported experiments are interesting but as discussed below key conclusions are based on non-physiological genetic perturbations (overexpression) and several experiments do not include controls necessary for interpretation of the results, tempering my enthusiasm for the manuscript. It is possible that some of the needed data are already in hand but not shown. With some additions and a more tempered interpretation of the results, I'd be happy to take another look at this study.

Major points.

1. "Gyp7 localizes to endosomes." [line 142] The authors show that overexpressed Gyp7 localizes to punctate structures that appear to label with the endocytic tracer FM4-64. However, no co-localization with known protein markers of endosomes is shown, except to a limited extent in a vps4Δ background, where dozens of markers accumulate at class E compartments. This is an odd omission. Moreover, the authors see *more* localization of Gyp7 to punctate structures when Rab5 or Rab5 effector function is impaired, not less - and these punctae do not seem to be marked by FM4-64. It is hard to see this as support for the hypothesis that Gyp7 localizes to endosomes. Could these be, for example, Atg8 accumulations rather than endosomes?

Reviewer 1 had similar points, and we have not identified the identity of Gyp7 puncta yet. We tested colocalization with many endosomal markers and Atg8, but did not find any significant colocalization. Even by time-lapse imaging, we were unable to find colocalization. However, Gyp7 accumulates in Class E endosomes if vps4 is deleted. This observation is quite similar to the behavior of the GEF Vps9, which is mainly cytosolic, and only found in endosomes under these conditions. In addition, overexpressed Gyp7 colocalizes strongly with Mon1-Ccz1, next to Ypt7 puncta, suggesting an endosomal origin also of this structure. We speculate that the Gyp7-positive puncta in wild-type cells might correspond to Rab5-deficient endosomal structures.

2. "Relocalization of Gyp7 to vacuoles impairs vacuole morphology." [line 178] This is a reasonable conclusion on the basis of overexpression as previously reported and experiments shown here (Fig. 2A,B). However, the re-targeting experiments (Fig. 2C,E) show much larger effects for the affinity-tagged Vac8-CB used as an anchor to relocalize Gyp7 than for the relocalization itself. Or perhaps I'm misreading the experiment? I asked two other experienced people in my lab to read this section of the paper, and they read it the same way. I don't see how this experiment can be interpreted using a background with what seems to be a reasonably strong vac8 hypomorph.

We understand the reviewer's concern regarding this experiment since chromobody-fused Vac8 seems to have partially impaired function. Therefore, we repeated the experiment with the chromobody fused to Zrc1, a vacuolar membrane zinc transporter, as an additional readout for vacuolar recruitment of Gyp7. Here, the number of vacuoles does not increase upon simple tagging of Zrc1 with the chromobody, while recruitment of Gyp7 to the vacuole via Zrc1-CB causes a strong vacuolar morphology defect. Thus, we replaced the microscopy data of chromobody-fused Vac8 with chromobody-fused Zrc1 (Fig. 2C-E).

Additionally, it's hard to see how expression of a presumptively spontaneous nucleotide-exchanging variant of Ypt7 is a better control here than a catalytic-dead Gyp7 (R458K), as used in previous studies (Eitzen, EMBO J 2000; Brett, JCB 2008). Use of this well-characterized mutant could have strengthened several experiments in the present study. It's perplexing that R458K was not employed in this study.

We appreciate the reviewer's suggestion. In addition to the expression of the Ypt7^{K127E} in the Gyp7-GFP Zrc1-CB background (Fig. 2D,E), we included expression of the catalytic-dead Gyp7 in our relocalization experiments. Importantly, we are able to show that recruitment of Gyp7^{R458K}-GFP to neither the vacuole (Zrc1-CB) or endosomes (Vps8-CB) affects vacuole morphology (Fig. 2F,G). Therefore, our data provides evidence that relocalization of functional Gyp7 to the vacuole and thus GAP-mediated Ypt7 inactivation impairs vacuole morphology.

3. "Gyp7 is required for homeostasis of the endosomal system."[line 204] The authors show data suggesting that perturbation of Gyp7 function alters TORC1 signaling, consistent with the known role of endolysosomal traffic in the TORC1 pathway. It is interesting that an msb3 (Rab5 GAP) mutant phenocopies the gyp7 deletion for this readout.

Data are also shown suggesting that traffic kinetics through the endosomal MVB pathway to

the vacuole are (very) subtly regulated by Gyp7 activity. The experiments do not clearly delineate whether the target of this regulation is Ypt7 residing on the endosome, on the vacuole, or both.

We agree with the reviewer that our experiments do not clearly distinguish which pool of Ypt7 is primarily targeted by Gyp7. However, Gyp7 is only found in puncta and not on the vacuolar membrane, even upon overexpression of the protein, which shifts a Ypt7 pool from the vacuole to endosomes (Fig. 6A,B). Therefore, it is likely that Gyp7 acts on the endosomal Ypt7 pool.

4. "Gyp7 activity depends on the membrane environment." [line 232]. It is persuasively shown that Gyp7 binds membranes, that it prefers to bind membranes with a vacuole-like membrane mixture (an endosomal vs. vacuole lipid mixture was not tested, as might have been expected given the overall argument of the paper), and that this activity depends on a PH-like domain near the protein's N-terminus. The PH-like domain alone does not bind membranes in the experimental configurations employed.

The authors use mainly GDI extraction as a proxy for Gyp7 activity against Ypt7/Rab7. There's nothing wrong with this approach, as such. But curiously direct assay of Ypt7 GTPase activity is reported solely in Fig. 5J. The authors claim that this shows allosteric regulation of Gyp7 activity against soluble (non-lipidated) Ypt7 by membranes. The result shows a very small but apparently reproducible difference in activity. But given the advantages of a chemically defined system, why was GTPase activity not assayed directly throughout? This is not hard to do using well-described colorimetric, fluorescence, or [32]P orthophosphate release assays, or presumably the HPLC assay in Fig. 5J.

Given the absence of direct readouts of GTP hydrolysis, it is important to test whether the lipid mix used (VML vs. PC/PE) influences the ability of GDI to extract Ypt7-GDP. This control is important if extraction is used as the main proxy for the Rab's nucleotide state. Also, it was not clear to this reader whether GDI is present in excess to Ypt7, or what the final GDI concentration was in the extraction experiments.

We agree with the reviewer that it is an important control to show whether GDI is able to extract Ypt7-GDP from PC/PE liposomes. In our normal experimental setup, the molar ratio between Ypt7 and GDI is 1:1 (600 nM each). Now we provide data, which show that a 10x excess of GDI (6 µM) does not lead to further extraction of Ypt7 either bound to VMLs or to PC/PE liposomes (Fig. S3). Furthermore, we analyzed the extraction of Ypt7 from liposomes after incubation with the catalytically active TBC domain of Gyp1 (Gyp1-46), which does not rely on membranes for its activity (Fig. 4L,M). Here, we observed no difference in GDI-mediated extraction of Ypt7 from VMLs vs. PC/PE liposomes, indicating that GDI in principle is able to extract Ypt7-GDP from both VMLs as well as from PC/PE liposomes. Together, the data show that the function of Gyp7 but not of GDI depends on the membrane composition.

Overall, the experiments support the idea that direct membrane association increases Gyp7 activity against Ypt7. They do not strongly support the idea that membrane association has a major allosteric effect on Gyp7 catalytic activity.

We agree with the reviewer's comment and adjusted the text accordingly. We currently do not know how the membrane composition influences Gyp7 activity, and we can only speculate here.

5. "Gyp7 activity confines Ypt7 to late endosomes and signaling endosomes." Taken literally, this is obviously wrong, since Ypt7 on vacuoles is needed for vacuole fusion, as exhaustively demonstrated by many labs including the authors', and the data show (as entirely expected) lots of Ypt7 on the vacuole in wild type cells. Fig. 6A also shows that overproduction of Gyp7 removes Ypt7 from the vacuole, and if anything, increases its localization to (presumptively) endosomal punctae. This would seem to argue that Gyp7 preferentially targets Ypt7 on the vacuole, not on the endosome as the authors suggest earlier in the manuscript.

The reviewer is right; the statement is not quite correct and misleading. We meant to say that the pool of Ypt7 is shifted from a primary vacuole localization to a strongly confined endosomal pool. As Gyp7 only found in puncta and not at the vacuolar rim, we interpret this in favor of an inactivation of Ypt7 here in endosomal compartments rather than on the vacuole. Of course, we cannot exclude an additional role of Gyp7 on the vacuole, which may escape our detection. We therefore discussed this issue in more detail in the manuscript.

Other experiments here are based on a truncation of the GEF subunit Mon1 that results in elevated Ypt7 activity, as nicely shown in recent work from the same group. But Gyp7 is not shown to colocalize with Mon1 or Ypt7 under these circumstances. An interesting observation is that endosomes marked by Pep12 increase in number in a MON1Δ100 mutant that also overproduces Gyp7. However, it's not tested whether this phenotype is due to one of these genetic manipulations, or both (Fig. 6E).

Importantly, the overall number of Pep12 puncta per cell does not increase but decrease, while the number of Pep12 puncta, which do not colocalize with the vacuole, significantly increases (see Fig. 7C,D, Fig. S6B). However, we agree with the reviewer and further dissected whether one or both genetic manipulations cause this phenotype. Interestingly, we find that overproduction of Gyp7 leads to the overall decrease of Pep12 puncta and their localization distant from the vacuole. Expression of the truncated and hyperactive GEF causes a slight, though significant decrease in the number of the same structures, while it does not affect the subcellular distribution of Pep12 puncta. Thus, the data suggest that Gyp7 does not only affect Ypt7 localization and TORC1 activity but is rather important for the overall endosomal system organization/functioning.

Furthermore, we addressed the colocalization of Gyp7 with Mon1-Ccz1 and Ypt7 in wild-type cells as well as upon genetic manipulation of the Ypt7 GEF and GAP. We find that Gyp7 does not colocalize with Ypt7 puncta in both condition, whereas the colocalization of Gyp7 and the GEF subunit Ccz1 strongly increases upon overexpression of Gyp7 (Fig. 6C,D). This result suggests that the Ypt7 GEF and GAP indeed localize to the same endosomal compartment, while Ypt7 shifts from a vacuolar to an endosomal population. Importantly, overexpressed Gyp7 does not localize and inactivate Ypt7 on the vacuole.

6. "Endolysosomal transport is delayed upon Ypt7 confinement to late endosomes." [line 338]. The delays are again subtle but apparently statistically significant, and consistent with

the ability of Gyp7 to deplete Ypt7 from the vacuole as shown in Fig. 6A.

We rephrased this part to make clear that this is a subtle defect. This is probably also expected for a regulator of Ypt7 activity such as a GAP.

7. "Ypt7-positive structures correspond to signaling endosomes." Immunogold EM shows that overproduced Ypt7 can be detected on endosomal structures, and Ypt7 accumulates on Class E compartments in a vps4Δ mutant (along with dozens of other endolysosomal proteins). In Fig. S6A,B a reporter system is used to assay endosomal vs. vacuolar phosphorylation of Sch9 by Tor1. In a gyp7Δ mutant vs. wild type, a significant decrease in TORC1 activity is seen at the vacuole and *not* at the endosome. Overproduction does increase signaling at the endosome, but given the lack of a deletion phenotype, this is not a strong argument for a normal physiological function of Gyp7 at the endosome per se. I wonder if stronger phenotypes would emerge in nitrogen limited conditions.

We appreciate the reviewer's suggestion, yet also disagree in part. The *gyp7*Δ mutant does not impair vacuole morphology, yet has a clear defect in Mup1 uptake and in TORC1 signaling. The phenotype is certainly not as drastic as a fusion mutant, which is also not expected, given that Gyp7 is a regulator of Ypt7. Nevertheless, we agree with the reviewer that the *gyp7*Δ mutant might show a stronger phenotypic response if cells are additionally challenged by nitrogen starvation. Therefore, we compared vacuole morphology of wild-type vs. *gyp7*Δ cells upon 2 h of nitrogen starvation (Fig. 3F-H). Again, *gyp7*Δ cells do not behave differently than wild-type cells in both growth conditions and upon nitrogen starvation. As suggested previously (Reviewer #1, comment 7), it is a reasonable possibility that upon loss of Gyp7 function another Ypt7 GAP might take over its function.

Minor issues.

8. The paper by Eitzen (EMBO J 2000) is not cited, and should be.
9. Line 216: In yeast, Apl5 is not an endosomal trafficking protein.
10. Line 224: Fig. 3C is not mentioned in the Results, so far as I can tell.
11. Fig. S2B: genotypes should be labeled.

We agree with the reviewer and addressed these issues.

- Alexey Merz

Reviewer #3 (Comments to the Authors (Required)):

In the present study, Füllbrunn et al. dissect the endocytic localization and function of the Ypt7 (RAB7) specific GAP protein Gyp7 in yeast. While Gyp7 is already known to be a GAP for RAB7, the precise localization and membrane dependency of Ypt7 inactivation through Gyp7 remained to be elucidated.

The authors demonstrate that Gyp7 localizes primarily to endosomes but not to the vacuole and that this localization partially depends on an intact Vps21 (RAB5) system. Additional localization experiments indicate that Gyp7 functions on endosomes but likely not on the

vacuolar membrane. Deletion of Gyp7 delayed endosomal transport towards the vacuole and altered endosomal mTORC1 signaling, suggesting that Gyp7 is required for the homeostasis and signaling function of endosomes. In an additional line of experimentation, the authors demonstrate that Gyp7 requires endosomal membranes for its GAP activity as membrane free Gyp7 was hardly active towards Ypt7. Finally, the authors demonstrate that Gyp7 activity confines Ypt7 to late endosomes which are also signaling endosomes.

Overall, the data is of high quality and the authors' conclusions appear reasonable to this reviewer. The authors thoroughly dissect the localization of Gyp7, its effect on Ypt7 and its role within the endocytic network. With this being said, I think that the manuscript is somewhat uninspiring as Gyp7 was already known to be the dominant Ypt7 GAP protein in yeast . It is still a solid and thorough cell biological analysis of a previously known RAB7 GAP in yeast but it doesn't add a lot of groundbreaking insight into the function of this endocytic protein. While I am generally supportive of publication I am not sure whether JCB is an appropriate venue for this manuscript.

We respectfully disagree with the reviewer's opinion on the suitability of our manuscript for JCB. The manuscript addresses here the role of a GAP in controlling the Rab7 function by taking both functional assays (GAP assays, GAP relocalization, TORC1 activity measurements) and *in vivo* analyses into account. The results of this analysis show that Gyp7 controls Ypt7 function and consequently a pool of late endosomes, for which we have coined the name signaling endosomes. What is most surprising is the strong effect of Gyp7 overproduction on expanding the Ypt7 pool proximal to the vacuole (Ypt7 puncta), and subsequently altering TORC1 signaling. This suggests that Gyp7 functions at an endosomal compartment and controls Ypt7 function here. This analysis is, as the other two reviewers also agree with, novel and unexpected and thus within the general scope of JCB.

Minor points:
Figure 4A: "floatation" seems odd

We corrected this.

The GTPase activating protein Gyp7 regulates the activity of the Rab7-like Ypt7 on late endosomes

Nadia Füllbrunn[1,2], Raffaele Nicastro[3], Muriel Mari[4], Janice Griffith[5], Eric Herrmann[6], René Rasche[6], Ann-Christin Borchers[1], Kathrin Auffarth[1], Daniel Kümmel[6], Fulvio Reggiori[4,5], Claudio De Virgilio[3], Lars Langemeyer[1,2*], Christian Ungermann[1,2*]

[1] Osnabrück University
Department of Biology/Chemistry
Biochemistry section
49076 Osnabrück, Germany

[2] Center of Cellular Nanoanalytics (CellNanOS)
Osnabrück University
49076 Osnabrück, Germany

[3] University of Fribourg
Department of Biology
CH-1700 Fribourg, Switzerland

[4] Aarhus University
Department of Biomedicine
8000 Aarhus, Denmark

[5] University Medical Center Utrecht
Department of Cell Biology
3584 CX Utrecht, The Netherlands

[6] University of Münster
Institute of Biochemistry
48149 Münster, Germany

* Corresponding authors:
Email: lars.langemeyer@uos.de (L.L.), cu@uos.de (C.U.)
http://www.biochemie.uni-osnabrueck.de/
Phone: +49-541-969-2752

Running title: GAP control in Rab7 localization and function

Abstract

Organelles of the endomembrane system contain Rab GTPases as identity markers. Localization of Rab GTPases is determined by specific activating guanine nucleotide exchange factors (GEFs) and GTPase activating proteins (GAPs). It remains largely unclear, however, how these regulators are specifically targeted to organelles and how their activity is regulated. Here, we focus on the GAP Gyp7, which acts on the Rab7-like Ypt7 protein in yeast, and surprisingly observe the protein exclusively in puncta proximal to the vacuole. Mistargeting of Gyp7 to the vacuole strongly affects vacuole morphology, suggesting that endosomal localization is needed for function. In agreement, efficient endolysosomal transport requires Gyp7. *In vitro* assays reveal that Gyp7 requires a distinct lipid environment for membrane binding and GAP activity. Overexpression of Gyp7 concentrates Ypt7 in late endosomes, and results in resistance to rapamycin, an inhibitor of the target of rapamycin complex 1 (TORC1), suggesting that these late endosomes are signaling endosomes. We postulate that Gyp7 is part of a regulatory machinery involved in late endosome function.

Keywords: Gyp7, Ypt7, GAP, Rab GTPase, endosome, lysosome

Introduction

Maintaining membrane integrity and organelle homeostasis requires intracellular transport between organelles, which occurs via vesicular transport or membrane contact sites. During vesicular transport, proteins are concentrated in forming vesicles. These pinch off from a donor membrane and fuse with an acceptor membrane. Fusion of vesicles relies on a whole set of proteins, termed the fusion machinery, including SNAREs, tethering factors and Rab GTPases.

Rab GTPases (Rabs) are key identity markers of endomembranes (Müller and Goody, 2018; Borchers et al., 2021; Barr, 2013; Hutagalung and Novick, 2011). They function as molecular switches and exist in an active GTP-bound and an inactive GDP-bound form. Rabs require specific guanine nucleotide exchange factors (GEFs) for their GTP loading and GTPase activating proteins (GAPs) for their inactivation. Rabs exist in the cytosol in complex with the chaperone-like guanine nucleotide dissociation inhibitor (GDI) and randomly associate with membranes via their C-terminal prenyl anchor. If they encounter their GEF, it promotes nucleotide exchange of GDP for the more abundant GTP by destabilizing the nucleotide binding pocket, which triggers loading with the more abundant GTP and stable membrane association. In this active, membrane-bound form, Rabs interact with effectors, such as tethering factors to mediate fusion. As Rabs are inefficient enzymes (Müller and Goody, 2018), GAPs are required to trigger GTP-hydrolysis. The Rab-GDP is subsequently extracted by GDI from membranes, thus completing the Rab cycle.

Along the endolysosomal pathway, Rab5 and Rab7 define organelle identity of early and late endosomes and lysosomes by coordinating membrane fission and fusion processes (Borchers et al., 2021). Endocytic vesicles deliver their cargo to Rab5-positive endosomes. These endosomes change in morphology by sorting cargo into intraluminal vesicles with support of the ESCRT complexes, which results in the formation of multivesicular bodies (MVBs) or late endosomes, while other proteins are rerouted into retrograde tubules (McNally and Cullen, 2018; Vietri et al., 2020). In yeast, endosomes accumulate in a prevacuolar compartment proximal to the vacuole (Day et al., 2018). In addition, a subpopulation of endosomes, signaling endosomes, has been described, which carry a fraction of the otherwise vacuolar target of rapamycin complex 1 (TORC1) (Hatakeyama et al., 2019).

During endosome maturation, Rab5 (Vps21 in yeast) is replaced for Rab7 (Ypt7 in yeast) (Borchers et al., 2021; Rink et al., 2005; Poteryaev et al., 2010). This process seems to occur in a sharp transition, which is likely driven by Rab5 levels. These may activate the Rab7-GEF and recruit Rab7 to membranes. In turn, Rab7 may trigger Rab5 release by recruiting the corresponding Rab5 GAP. Mathematical modelling suggests that the crosstalk of GEF and GAP with the involved Rabs determine this transition (Conte-Zerial et al., 2008; Barr, 2013).

This transition may be further tuned by corresponding Rab effectors. First reconstitution assays of the Rab5 GEF cascade together with Rab5 effectors showed strongly confined Rab5-positive zones on membranes (Bezeljak et al., 2020; Cezanne et al., 2020).

The conserved Mon1-Ccz1 complex was identified as the Ypt7 GEF complex in yeast (Nordmann et al., 2010) and subsequently in human cells (Gerondopoulos et al., 2012). Mon1-Ccz1 is a Vps21/Rab5 effector (Li et al., 2015; Cui et al., 2014; Langemeyer et al., 2020; Singh et al., 2014; Kinchen and Ravichandran, 2010). We showed before that Vps21 both recruits and activates Mon1-Ccz1 on membranes (Langemeyer et al., 2020). This process is further enhanced by the membrane environment, which the complex samples (Herrmann et al., 2023), and allows Mon1-Ccz1 to target both to endosomes and autophagosomes (Gao et al., 2018; Hegedűs et al., 2016; Herrmann et al., 2023). In *Drosophila* and human cells, the GEF complex contains a third subunit, whose loss results in strong autophagy and endosomal defects and lysosomal cholesterol accumulation (Vaites et al., 2018; Dehnen et al., 2020; Boomen et al., 2020).

Yeast Mon1-Ccz1 is an endosomal complex (Gao et al., 2022, 2018), yet Ypt7 is required both on endosomes and the vacuole to promote recycling and fusion. Ypt7 has several effector proteins. Ypt7 binds the retromer complex, which is involved in membrane protein recycling (Liu et al., 2012; Balderhaar et al., 2010; Purushothaman et al., 2017). It also interacts with the inverted BAR protein Ivy1, a protein involved in signaling at endosomes and activity control of the Fab1 lipid kinase complex, which generates phosphatidylinositol-3,5-bisphosphate ($PI(3,5)P_2$) (Numrich et al., 2015; Varlakhanova et al., 2018; Malia et al., 2018). Finally, Ypt7 interacts with the HOPS tethering complex, which is required for SNARE-mediated membrane fusion of endosomes, autophagosomes and Golgi-derived AP-3 vesicles with the vacuole (Shvarev et al., 2022; Wickner and Rizo, 2017).

Less is known about the GAP-mediated inactivation of Ypt7. Almost all GAPs have a central Tre/Bub2/Cdc16 (TBC) domain with a catalytic arginine-glutamine finger (Albert et al., 1999). These fingers complete the nucleotide binding site of a Rab and thus allow for GTP hydrolysis (Pan et al., 2006). Although Gyp7 has been one of the first identified GAPs, its substrate specificity remained unclear as the *in vitro* activity revealed low substrate specificity (Vollmer et al., 1999; Albert et al., 1999; Lachmann et al., 2012). However, Gyp7 seems to act on Ypt7 as its overexpression results in Ypt7 inactivation and vacuole fragmentation *in vivo* (Brett et al., 2008). Furthermore, Gyp7 can inhibit vacuole-vacuole-fusion at the docking stage *in vitro* (Eitzen et al., 2000).

Yeast encodes for eight GAPs, but 11 Rabs, though the specificity of these GAPs to their Rab remains unclear. To inactivate Rabs, GAPs may decode the membrane by binding to specific

proteins and/or recognize specific phosphoinositides. These interactions can occur as part of a Rab cascade, where the downstream Rab recruits the GAP of the upstream Rab (Barr, 2013). For mammalian Rab7, the four GAPs Armus/TBC1D2A, TBC1D2B, TBC1D5 and TBC1D15 have been identified. All indeed recognize membranes via lipid-binding motifs, coiled-coil motifs or LC3-interacting regions (Stroupe, 2018; Popovic and Dikic, 2014; Kanno et al., 2010; Frasa et al., 2010; Jia et al., 2016; Zhang et al., 2005; Peralta et al., 2010). Most Rab7 GAPs function in autophagy, while TBC1D5, together with the retromer complex, specifically restricts Rab7 to endosomal microcompartments and affects signaling processes and endosomal maturation (Jimenez-Orgaz et al., 2018; Kvainickas et al., 2019).

Although Gyp7 has been identified as the only Ypt7-specific GAP, it remains unclear how and when Gyp7 inactivates Ypt7. We therefore set out to analyze Gyp7 function in detail. Here, we show that Gyp7 localizes in dot-like structures next to the vacuole, suggesting that they are of endosomal origin. Using *in vitro* assays, we demonstrate that Gyp7 has high affinity for membranes, which enhances its GAP activity for membrane-bound Ypt7. We further show that Gyp7 overproduction can retain Ypt7 on late endosomes, which enhances endosomal TORC1 signaling. These Ypt7-positive endosomes lack ESCRTs, yet require ESCRTs for their formation. We thus speculate that these late endosomes correspond to signaling endosomes.

Results

Gyp7 localization depends on an intact endosomal system

In yeast, Ypt7 functions in multiple fusion and fission reactions at the vacuole as well as in formation of vCLAMPs, the membrane contact site between vacuoles and mitochondria (Fig. 1A). To clarify the Ypt7 pool targeted by Gyp7, we tagged Gyp7 C-terminally with mNeonGreen and determined its localization by fluorescence microscopy. We observed Gyp7 in single puncta proximal and peripheral to the vacuole (Fig. 1B). Gyp7 was strongly concentrated in the so-called Class E compartments, which were also stained by the lipophilic dye FM4-64, upon inactivation of the ESCRT-IV subunit Vps4 (Babst et al., 1998) (Fig. 1B). Here, Gyp7 colocalized with other endosomal proteins such as the Rab5-like Vps21 and the retromer subunit Vps35 (Fig. 1C, D). In contrast, Msb3, the previously identified GAP of Vps21 that shows some GAP activity for Ypt7 as well (Lachmann et al., 2012), was not enriched in this compartment (Fig. 1B).

To determine, whether specific endosomal proteins are required for Gyp7 localization, we analyzed several mutants (Fig. 1E, F, Fig. S1A), including deletions of the major Rab5 proteins Vps21 and Ypt52, their corresponding GEFs Vps9 and Muk1, respectively, the CORVET

subunit Vps3, the endosomal Sec1/Munc18-like Vps45, the endosome-specific subunit of the phosphatidylinositol 3-kinase Vps34 (*vps38*Δ), and several proteins involved in endosomal retrograde transport (*snx4*Δ, *vps5*Δ, *vps35*Δ, *mvp1*Δ). None of these mutants abolished the distribution in puncta of Gyp7 completely. However, all impairing mutants of fusion proteins in the endosomal system, such as *vps21*Δ *ypt52*Δ, *vps3*Δ or *vps45*Δ, had more than 5-times more Gyp7 puncta, which predominantly were localized more distal from the vacuole (Fig. 1E). This could be either explained by disruption of Gyp7 recruitment or an overall alteration of endosomal morphology per se. Furthermore, among all proteins involved in membrane recycling, only *MVP1* deletion caused a reduction in Gyp7 puncta. Similar observations were made for *ypt52*Δ and *ypt53*Δ cells. Our data suggest that Gyp7 recruitment does not depend on the presence of single endosomal proteins but on an intact endosomal system.

We also analyzed the influence of Gyp7 on Ypt7 function in autophagy and vCLAMP formation. Neither *GYP7* deletion nor its overexpression altered transport of the autophagy-specific Atg8 protein to the vacuole lumen upon starvation (Fig. S1B-D). We noticed, however, that overexpression of Gyp7 resulted in slightly more Atg8-positive puncta in growth conditions (Fig. S1C). To follow vCLAMPs, we overexpressed mCherry-tagged Vps39, which accumulates in wild-type cells between vacuoles and DAPI-stained mitochondria (Fig. S1E, F). Again, manipulation of Gyp7 expression levels had no effect. In addition, Gyp7 did not localize to vCLAMPs.

We conclude that any deletion of key endosomal proteins results in multiple Gyp7-positive puncta, yet no release of Gyp7 from membranes. This suggests that Gyp7 recruitment to the endolysosomal system occurs independent of the analyzed endosomal proteins.

Relocalization of Gyp7 to vacuoles impairs vacuole morphology

A major pool of Ypt7 is found on the vacuolar rim, while Gyp7 localizes in dot-like structures of the endolysosomal system. Nevertheless, overexpression of Gyp7 from the *GAL1* promoter can trigger vacuole fragmentation (Fig. 2A, B) (Brett et al., 2008). This suggests that Gyp7-mediated inactivation of Ypt7 strongly impairs vacuole morphology.

To determine whether Gyp7 dynamically localizes to both vacuoles and endosomes to control Ypt7 activity, or functions exclusively at endosomes, we tagged the endosomal CORVET subunit Vps8 or the vacuolar zinc transporter Zrc1 with a nanobody against GFP (chromobody, CB) in strains expressing endogenous Gyp7-GFP, an approach we previously established to confine proteins at specific subcellular locations (Malia et al., 2018). We first analyzed vacuole morphology of strains exclusively expressing Vps8-CB or Zrc1-CB and observed no effect on vacuole morphology, indicating that tagging Vps8 or Zrc1 does not impair their functionality (Fig. 2C, E). We then turned to strains that additionally expressed Gyp7-GFP or the catalytic

dead version of Gyp7-GFP, Gyp7^{R458K}. Sequestering Gyp7 or Gyp7^{R458K} to endosomes via Vps8-CB confined these variants to single puncta, and vacuoles looked like wild-type (Fig. 2D-G). In contrast, relocalizing Gyp7 but not Gyp7 ^{R458K} to the vacuole via Zrc1-CB strongly fragmented vacuoles. This indicates that Gyp7, which was present in multiple puncta at the vacuole, inactivated Ypt7 here.

To exclude that the artificial confinement of Gyp7 to the vacuole via Zrc1-CB caused a non-specific effect on vacuole fusion or fission, we expressed the Ypt7^{K127E} mutant in this background. Ypt7^{K127E} has a fast nucleotide exchange and can bypass the Ypt7 GEF requirement and possibly also the requirement for the GAP (Kucharczyk et al., 2001; Cabrera and Ungermann, 2013). Indeed, Ypt7^{K127E} expression completely rescued the vacuole morphology, indicating that the previously observed vacuole fragmentation was caused by Ypt7 inactivation at the vacuolar membrane. Our observations thus agree with a major functional role of Gyp7 at endosomes, and not at the vacuole.

Gyp7 is required for homeostasis of the endosomal system

To analyze the role of Gyp7 in endosomal functions, we analyzed cells lacking *GYP7* in growth and endocytosis assays. For growth assays, we spotted cells in serial dilutions on plates containing 4 mM Zn^{2+}, a stressor of the endosomal pathway (Fig. 3A). Here, we observed a slight growth defect of *gyp7*Δ, which was comparable to the one of *vps21*Δ cells. Deletion of the Vps21 GAP Msb3 was even more deficient, suggesting that Gyp7 is as important for a functional endosomal pathway as normal Vps21 activity. We also analyzed whether Gyp7 is required for normal function of the target of rapamycin complex 1 (TORC1), which localizes to signaling endosomes and lysosomes (Hatakeyama and Virgilio, 2019; Hatakeyama et al., 2019) (Fig. 3B). TORC1 is sensitive to the inhibitor rapamycin, and sensitivity of cells to this drug indicates defective targeting and/or function of this complex. Like *msb3*Δ and *tor1*Δ cells, yeast cells lacking Gyp7 were sensitive to rapamycin. Similarly, cells with deletions of proteins involved in endosomal recycling (*vps35*Δ, *vps5*Δ) or Golgi-to-vacuole trafficking (*apl5*Δ) showed comparable sensitivity to rapamycin, whereas cells expressing a non-phosphorylatable Fab1 mutant are resistant to rapamycin (Chen et al., 2021) (Fig. S2A). Importantly, tagging of Gyp7 with either mNeonGreen or GFP was without effect on growth, indicating that this modification does not interfere with its function (Fig. 3A, B). Thus, Gyp7 function affects TORC1 function within the endolysosomal system.

To analyze the role of Gyp7 in endocytosis, we followed the transport of the methionine transporter Mup1-GFP in wild-type and *gyp7*Δ cells. In the absence of methionine, Mup1 accumulates at the plasma membrane (Fig. 3C). Once methionine is added, Mup1 is endocytosed and transported via endosomes to the vacuole lumen. The initial uptake of Mup1

and delivery to endosomes at early time points upon methionine addition was comparable in both tested strains (Fig. S2B, C). In contrast, *gyp7*Δ cells showed a clear delay in Mup1 delivery to the vacuole at later time points, i.e., 20-30 min post methionine addition, which was reflected by a decreased vacuole/plasma membrane Mup1 intensity ratio and more endosomal Mup1 (Fig. 3D, E). Overall, we conclude that Gyp7 is required for efficient endocytosis and thus endosomal functions.

Gyp7 activity depends on the membrane environment

To understand Gyp7 function and GAP activity in more detail, we adapted a simple *in vitro* assay to our necessities (Thomas et al., 2021). Liposomes with a vacuole mimicking lipid (VML) composition (Zick and Wickner, 2014a) were incubated with prenylated Ypt7 in complex with GDI in the presence of EDTA, GTP and $MgCl_2$ (see Methods). Under these conditions, prenylated Ypt7 is chemically activated and loaded with GTP, and thus becomes resistant to free GDI (molar ratio of GDI to Ypt7 is 1:1) unless its bound GTP is hydrolyzed to GDP with the help of a GAP. To determine the membrane-bound fraction of Ypt7, liposomes are floated in a sucrose gradient, before analyzing the input and floated material by Western blotting (Fig. 4A). In the absence of a GAP, Ypt7 was anchored to liposomes and not extracted by GDI. In the presence of increasing amounts of full-length Gyp7, corresponding to a molar ratio of 1:20,000 to 1:32 (Gyp7 to Ypt7), Ypt7 was efficiently inactivated and extracted by GDI as shown by the decreasing amount of Ypt7 in the floated fraction (Fig. 4B, C). We initially incubated samples for 1 h. To analyze the kinetics of Gyp7, as determined by GDI extraction, we incubated reactions containing 0.75 nM Gyp7 for different time points, and then observed the membrane association of Ypt7 (Fig. 4D, E). Our data revealed that 20 min were sufficient for almost 90% of Gyp7-mediated GTP-hydrolysis on Ypt7. Unless indicated otherwise, we incubated Ypt7-liposomes with 3.75 nM Gyp7 for 10 min in the following experiments to allow for efficient inactivation and membrane removal of Ypt7.

To determine whether Gyp7 associated with membranes, we added Gyp7 to liposomes and analyzed binding to membranes in a simple liposome sedimentation assay (Fig. 4F, G). Gyp7 strongly pelleted in liposome-containing samples indicating that it binds membranes, while pelleting of Gyp7 in the absence of liposomes resulted in negligible background. The VML mixture of our liposomes contains a complex lipid mixture of 47 mol% phosphatidylcholine (PC), 18 mol% phosphatidylethanolamine (PE), 18 mol% phosphatidylinositol, 1 mol% phosphatidylinositol-3-phosphate, 4.4 mol% phosphatidylserine, 2 mol% phosphatidic acid, 1 % diacylglycerol and 8% ergosterol. All lipids were dually unsaturated in both acyl chains (dilinoleoyl, 18:2). We asked if a simpler mixture of 82 mol% DLPC and 18 mol% DLPE would have the same effect. However, Gyp7 was completely inactive in our assay (Fig. 4H, I), as it did not bind to the membranes efficiently (Fig. 4 J, K). Importantly, association of Ypt7 with

membranes was unaffected by the liposome composition (Fig. 4H). Inefficient GAP activity of Gyp7 could thus be simply explained by its poor membrane binding.

To confirm that GDI is not limiting in our assay and able to extract Ypt7-GDP from PC/PE liposomes, we added 10-fold more GDI to our reactions (Fig. S3A, B). We observed similar levels of Ypt7 extraction on VMLs either in the absence or presence of excess GDI, suggesting that the GDI available in solution was sufficient to extract all Ypt7-GDP from membranes as soon as it became available during our assay (Fig. S3A, B). Importantly, addition of excess GDI did not significantly decrease the amount of Ypt7 bound to PC/PE liposomes, indicating that GDI is not limiting in our assay. Furthermore, we took advantage of the catalytically active TBC domain of Gyp1 (Gyp1-46), which was previously described to nonspecifically target Ypt7 among several other Rabs in solution and does not rely on membranes for its activity (Brett and Merz, 2008; Eitzen et al., 2000). Upon titration of Gyp1-46 instead of Gyp7 into our assay, we observed GAP activity towards membrane-bound Ypt7, followed by GDI extraction, on VMLs as well as on PC/PE liposomes, suggesting that GDI is in principle able to extract Ypt7-GDP from both VMLs and PC/PE liposomes (Fig. 4L, M). Interestingly, more than 1000-fold more Gyp1-46 was required to achieve comparable Ypt7 inactivation and membrane extraction compared to Gyp7 on VMLs (Fig. 4D, E), indicating that Gyp7 is highly specific for Ypt7. Together, we conclude that Gyp7 but not GDI depends on the right membrane composition for function.

To ask whether the membrane has additional functions beyond Gyp7 recruitment, we took advantage of the N-terminal His-tag of Gyp7 and generated liposomes containing the lipid DOGS-NTA, which can recruit His-tagged proteins to membranes (Cabrera et al., 2014). When present in liposomes containing just PC and PE, we now had sufficient Gyp7 on liposomes (Fig. 5A, B), yet did not significantly recover activity of Gyp7 (Fig. 5C, D). Importantly, DOGS-NTA had no negative impact on the Gyp7 GAP activity as Gyp7 shows comparable inactivation of Ypt7 on liposomes with the VML mixture lacking or containing DOGS-NTA (Fig. 4B, Fig. 5D). Together, our observations suggest that Gyp7 requires correct positioning and orientation on membranes, possibly by a distinct membrane environment, for full activity.

To identify the corresponding membrane-interacting region, we analyzed the Gyp7 model. According to the AlphaFold prediction (Fig. S4A, B), Gyp7 has an N-terminal PH domain (Fidler et al., 2016), a connecting middle domain and the catalytic TBC domain toward the C-terminal (Fig. 5E). The N-terminal PH domain with two positively charged patches and the middle domain with a potential amphipathic helix are possible Gyp7 regions involved in membrane binding. To search for a minimal membrane binding domain, we generated C-terminal truncations that contain just the predicted PH domain of Gyp7 (Fig. S4C), and observed no binding to liposomes (Fig. S4D, E). Likewise, the minimal GAP domain of just the TBC domain

of Gyp7 (Fig. 5E) had poor activity on membrane-bound Ypt7 compared to the full-length protein (Fig. 5H, I), as it did not bind to membranes efficiently (Fig. 5F, G), indicating that full-length Gyp7 is required for recognition and binding of membranes.

To ask whether the missing membrane recruitment causes the reduced GAP activity of the TBC domain towards membrane-bound Ypt7 or whether the membrane could have a direct activating effect on the GAP activity itself, we turned to a HPLC-based GAP assay. Here, the GTPase is constantly chemically reloaded with nucleotide due to the presence of EDTA and $MgCl_2$ (Araki et al., 2021; Eberth and Ahmadian, 2009) (Fig. 5J, S4F). This approach allowed us to directly compare the inactivation of soluble, not-prenylated Ypt7 by Gyp7 and the TBC domain in the absence or presence of liposomes (see Methods), and thus determine the role of the Gyp7 membrane association for Ypt7 inactivation. By following the amount of GTP left in the reactions over time (0, 10, 60, 180, 300 min), we determined the activity of our tested GAPs. In the absence of membranes, Gyp7 showed GAP activity towards Ypt7 over time. In line with our previous findings, this activity was only slightly increased in the presence of PC/PE liposomes, but significantly enhanced in the presence of liposomes with the VML composition (Fig. 5J). As expected, the presence of membranes did not affect the GAP activity of the TBC domain, as it did not bind membranes (Fig. S4F). Importantly, only background GTP hydrolysis occurred in samples without Ypt7, without GAP or neither Ypt7 nor GAP (Fig. S4G). Together, our data indicate that direct membrane association increases Gyp7 activity for Ypt7. As the GAP domain should be available for Ypt7, our data suggest that full-length Gyp7 recognizes the membrane-bound Ypt7 possibly at additional sites prior to its binding of the GTPase domain.

Gyp7 activity shifts Ypt7 localization from vacuoles to MVBs

Previous studies implied that high Gyp7 activity can remove Ypt7 from membranes if sufficient GDI is available (Cabrera and Ungermann, 2013). We also recently observed that the Ypt7 GEF Mon1-Ccz1 is hyperactive if the N-terminal part of Mon1 is truncated, i.e., $Mon1^{\Delta 100}$ (Borchers et al., 2023). Given that both Mon1-Ccz1 (Gao et al., 2018, 2022) and Gyp7 (as shown here) localize within the endolysosomal system, we wondered whether the levels or activity of the Ypt7 GEF and GAP could enhance endocytic trafficking as faster Ypt7 activation and turn-over would be expected. We initially followed Ypt7 localization in strains lacking or overexpressing Gyp7 from the *TEF1* promoter (Figure 6A, B). In wild-type cells, Ypt7 localizes to the vacuolar rim and in puncta proximal to the vacuole (Fig. 6A). As described, deletion of Gyp7 or Msb3, had no effect on Ypt7 localization, while the absence of both GAPs resulted in a slight, though significant, decrease in the number of Ypt7 puncta (Fig. S5A, B), indicating that other GAPs could take over the function of the main Ypt7 GAP Gyp7 upon its loss and under certain conditions. However, Gyp7 overexpression resulted in an increased number of

Ypt7 puncta and a fraction of Ypt7 puncta not proximal to the vacuole anymore. We repeated this analysis in a strain expressing Mon1$^{\Delta 100}$. This strain also accumulates more Ypt7 puncta, suggesting enhanced early to late endosome transition (Borchers et al., 2023). Deletion of Gyp7 did not affect this phenotype. However, overexpression of Gyp7 in the Mon1$^{\Delta 100}$ strain resulted in the same accumulation of Ypt7 puncta that now show increased fluorescence intensity and more Ypt7 puncta away from the vacuole (Fig. 6B). This suggests that Gyp7 can relocate Ypt7 from vacuoles to endosomes. We thus wondered how the Rab, the GEF and the GAP localize relative to each other (Fig. 6C). In wild-type cells and in the Mon1$^{\Delta 100}$ strain, Gyp7 does not colocalize with Ccz1, while overproduction of Gyp7 results in strong colocalization (Fig. 6D), suggesting that the Ypt7 GEF and GAP can indeed come together at the same endosomal compartment. However, these Gyp7-positive puncta did not colocalize with the Ypt7 puncta, even upon overproduction of the GAP (Fig. 6E), suggesting that active Ypt7 resides in a different endosomal compartment population. Overall, we suggest that Gyp7 activity shifts Ypt7 from a primary vacuolar localization to a subset of endosomes. Since Gyp7 is not present on vacuoles in any of our tested conditions, inactivation of Ypt7 might rather take place on endosomes, although we cannot exclude an additional role of Gyp7 at the vacuole or even elsewhere.

To determine the identity of the Ypt7 puncta under these conditions, we analyzed their colocalization with selected marker proteins. Ivy1 as a previously identified protein on signaling endosomes (Gao et al., 2022; Chen et al., 2021) strongly colocalized with Ypt7 puncta in Gyp7 overexpression strains, whereas colocalization with the retromer subunit Vps35 and the ESCRT protein Vps4 was mostly lost (Fig. 7A, B, S6A). We did not detect colocalization with the Vps21 protein. We then analyzed Pep12 as a Q-SNARE of endosomes and observed that the number of Pep12 puncta was slightly reduced in the Mon1$^{\Delta 100}$ strain and strongly reduced in the strain overexpressing Gyp7 (Fig. 7C, S6B). Moreover, several of these puncta were also more distant from the vacuole upon overproduction of Gyp7 and in combination with expression of Mon1$^{\Delta 100}$ (Fig. 7D, S6B), similarly to what we observed for Ypt7 puncta under the same conditions (Fig. 6A, B). However, no change in the localization of Tco89 as a TORC1 subunit was detected (Fig. 7E, S6C). These data indicate that the Ypt7 puncta correspond to mature late endosomes, i.e., MVBs, and/or signaling endosomes.

Ypt7 confinement to late endosomes affects protein traffic inbetween the endolysosomal system

To determine if the Ypt7 confinement due to Gyp7 overexpression affects transport toward the vacuole, we first analyzed the biosynthetic transport of carboxypeptidase 1 (Cps1) from the Golgi to the vacuole. In previous analyses, we observed that this transport is strongly delayed when Vps21 and the CORVET subunit Vps8 are overproduced. This manipulation causes the

arrest of endosomes with early endosomal markers, but not the vacuolar SNARE Vam3 or HOPS subunits, and results in the accumulation of Cps1 in puncta proximal to the vacuole (Fig. 8A-C) (Markgraf et al., 2009). However, Ypt7 confinement by Gyp7 overproduction in cells expressing Mon1$^{\Delta 100}$ resulted in similar localization of GFP-Cps1 as in wild-type cells (Fig. 8A-C).

We next analyzed the endocytic pathway toward the vacuole by monitoring Mup1-GFP transport upon methionine addition (Lin et al., 2008). To analyze the effect of altered Gyp7 or Mon1-Ccz1 activity, we followed Mup1-GFP trafficking at early time points (5, 10 min) after methionine addition (Fig. 8D, E). For each time point, we determined the ratio between the number of Mup1 puncta and the intensity of Mup1 signal in the plasma membrane. In strains overexpressing Gyp7, we observed a higher ratio at early time points of Mup1 uptake, while combining hyperactive Mon1-Ccz1 and overexpression of Gyp7 revealed the highest ratio (5, 10 min). In neither case, Mup1 was completely arrested on endosomes, but arrived at the vacuole lumen after 60 min. Together, the data indicate a slight delay of endocytic transport due to overexpressing Gyp7, as expected for a regulator of Ypt7 activity such as a GAP. We thus conclude that the confinement of Ypt7 impairs but does not block transport pathways to the vacuole.

Ypt7-positive structures correspond to MVBs

We previously showed that the formation of signaling endosomes as a subset of late endosomes requires both the ESCRT pathway and HOPS-mediated fusion of endosomes with vacuoles (Gao et al., 2022). One of the observations is that ESCRT and HOPS mutants are strongly impaired in TORC1 signaling (Gao et al., 2022; Zurita-Martinez et al., 2007). We therefore analyzed TORC1 activity in Gyp7 overexpressing strains. When grown on rapamycin to inhibit TORC1, cells lacking Gyp7 were clearly sensitive to this drug (Fig. 3B, S2A). In contrast, Gyp7 overproducing cells became slightly resistant to rapamycin, suggesting a likely higher TORC1 activity (Fig. 9A). This effect was also modestly enhanced in the presence of Mon1$^{\Delta 100}$. To resolve, which pool of TORC1 activity is mostly affected, we employed an established reporter assay, where the TORC1 target Sch9 localizes either to endosomes (endosomal TORC1, ET) or to the vacuole (vacuolar TORC1, VT) (Fig. S7A-B). ET and VT activity was then analyzed by monitoring the Sch9 phosphorylation on the ET or VT reporter using a phospho-specific antibody to the TORC1 target site on Sch9 (Hatakeyama et al., 2019). Importantly, we observed a clear decrease in VT activity in the *gyp7*Δ mutant, whereas ET activity was increased in the Gyp7 overproduction strain. The observations were less clear when overexpression of Gyp7 was combined with the Mon1$^{\Delta 100}$ mutant. This may be due to the Mon1$^{\Delta 100}$ allele causing a trafficking defect of the ET and VT probes as the endosomal

system is perturbed. All in all, we conclude that Gyp7-mediated confinement of Ypt7 to puncta next to the vacuole results in higher endosomal TORC1 activity.

We next asked whether the Gyp7-induced dot-like Ypt7 would accumulate in strains impaired in the ESCRT pathway, where the Class E compartment is found proximal to the vacuole. When Vps4 was deleted, mNeon-Ypt7 strongly accumulated in puncta proximal to the vacuole (Fig. 9B, top). This accumulation was likewise seen in the strain overproducing Gyp7 (Fig. 9B, bottom). Importantly, the endocytosed lipophilic dye FM4-64 also accumulated in these Ypt7-positive structures. This was not observed if Vps4 was present (Fig. 6A), indicating that the Ypt7 enriched endosomes allow efficient FM4-64 transport to the vacuole. The puncta localization of Ypt7 in *vps4*Δ cells is similar to previous findings, in which wild-type Ypt7 was overproduced in *vps4*Δ cells (Balderhaar et al., 2010). We thus concluded that Ypt7 puncta persist downstream of the formation of MVBs by ESCRTs.

All previous data suggest that Ypt7 is prominently present on MVBs, which accumulate upon overproduction of Gyp7 in our fluorescence microscopy data. We were wondering whether we could also observe an accumulation of MVBs in the mNeon-Ypt7 expressing strains by electron microscopy (Fig. 9C). In wild-type cells, single MVBs are occasionally found next to the vacuole. In the Mon1$^{\Delta 100}$ Gyp7 overproduction mutant, we detected MVBs with higher frequency throughout the cell sections and often organized in a cluster of 2-3 late endosomes, in line with the accumulation of Ypt7 puncta in this mutant. We then wondered if these structures may indeed carry Ypt7. Since the signal of endogenous Ypt7 is not sufficient for immuno-electron microscopy (IEM), we overproduced GFP-tagged Ypt7 in a wild-type background, which may mirror the endosomal effect of Ypt7 confinement by Gyp7 (Balderhaar et al., 2010). We analyzed the localization of overproduced GFP-tagged Ypt7 with nanoscale resolution in these cells by IEM. Immunogold-labeling of sections with an anti-GFP antibody revealed that Ypt7 was distributed on the vacuole membrane and even more prominently on multiple MVBs, which accumulated proximal to vacuoles (Fig. 9D). We thus conclude that Ypt7 functions on MVBs, which in part correspond to signaling endosomes. As Gyp7 can strongly confine Ypt7 proximal to the vacuole, we speculate that Gyp7 is a regulator of Ypt7 function at signaling endosomes.

Discussion

Within this study, we uncovered that the Ypt7-specific GAP Gyp7 localizes to puncta that correspond to compartments of the endosomal endosomal system, where it is needed for normal endolysosomal transport. In the absence of Gyp7, cells become sensitive to endolysosomal stresses and TORC1 inhibition. *In vitro*, Gyp7 membrane association and

activity is strongly regulated by the membrane environment. Surprisingly, Gyp7 overproduction does not liberate Ypt7 from endosomes, but rather confines it to a subpopulation proximal to the vacuole. This effect is even stronger in a strain also having hyperactive Ypt7 GEF due to the expression of the Mon1$^{\Delta 100}$-Ccz1 mutant complex. Under those conditions, cells become moderately resistant to the TORC1 inhibition. This subpopulation of Ypt7-positive endosomes require ESCRTs for their formation, yet lack Vps4, suggesting that they correspond to mature late endosomes/MVBs and are in part equivalent to signaling endosomes (Chen et al., 2021; Gao et al., 2022; Hatakeyama et al., 2019). Our data strongly suggests that Gyp7 regulates the function of these compartments.

Gyp7 is the Ypt7-specific GAP (Brett et al., 2008; Vollmer et al., 1999; Lachmann et al., 2012; Eitzen et al., 2000). However, deletion of Gyp7 has little effect on Ypt7 function, and vacuoles fragment only upon strong overexpression (Vollmer et al., 1999; Brett et al., 2008; Eitzen et al., 2000). We confirmed these findings and further show that mistargeting of endogenous Gyp7 to the vacuole membrane resulted in the same vacuole fragmentation phenotype. We can now explain the relatively minor effects of Gyp7 deletion on vacuole morphology as Gyp7 localizes to puncta proximal to the vacuole, presumably endosomes, and accumulates in late endosomes upon ESCRT deletion. In this regard, Gyp7 seems to function like mammalian TBC1D5 as a retromer-associated Rab7 GAP (Kvainickas et al., 2019; Jimenez-Orgaz et al., 2018). However, deletions of proteins involved in retrograde transport from endosomes did not completely abolish Gyp7 localization in puncta proximal to the vacuole. Only upon deletion of both Rab5-specific GAPs, Vps9 and Muk1, or other endosomal fusion proteins Gyp7 relocalized to multiple puncta (Fig. S1A). How Gyp7 is targeted to these structures, apart from binding to Ypt7, remains an open question at this point. It is, however, possible that Gyp7 binds specifically to endosomal membranes as artificial targeting of Gyp7 to more rigid membranes was not sufficient for its full activation *in vitro* (Fig. 5D).

Our analysis of Gyp7 uncovered a striking link between Ypt7 cycling and the formation of both mature late endosomes/MVBs and signaling endosomes. We previously showed that a subpopulation of endosomes harbors the TORC1 complex, which is otherwise found on vacuoles (Hatakeyama et al., 2019). These endosomes were thus named signaling endosomes. At this location, TORC1 phosphorylates the Fab1 complex and presumably modulates its activity (Chen et al., 2021). Additional factors involved in the biogenesis of the signaling endosomes are the HOPS and ESCRT complexes (Gao et al., 2022). Here, we discovered that enhanced Ypt7 cycling by Gyp7 overproduction and a hyperactive Mon1-Ccz1 complex confines Ypt7 to late endosomes. We postulate that these structures mature from Vps21-positive into Ypt7-positive late endosomes, a transition culminating with the loss of the ESCRT machinery (Fig. 9E). Even though MVBs may look phenotypically similar if arrested

early by overproducing Vps21 or Vps8 (Markgraf et al., 2009), or late by overproducing Ypt7 (Fig. 9D), they differ in their surface composition based on our analysis presented here. We therefore believe that the late, Ypt7-positive endosomes correspond in part to signaling endosomes as they are (i) positive for the specific marker protein Ivy1 (Numrich et al., 2015; Varlakhanova et al., 2018; Malia et al., 2018), (ii) contain the late endosomal SNARE Pep12, (iii) lack the ESCRT protein Vps4, (iv) require the ESCRT machinery for their formation, and (v) regulate endosomal TORC1 activity. As they are also reduced in their Vps21 content, these structures are likely matured Ypt7-positive MVBs as also suggested from our ultrastructural analysis of cells overproducing Ypt7 (Fig. 9C, D).

Why have these structures been overlooked? Ypt7 has been previously found in puncta proximal to the vacuole (Arlt et al., 2015; Balderhaar et al., 2010; Shimamura et al., 2019), which we interpreted as minor pool or a vacuolar domain. However, this may have been a misconception. As both Mon1-Ccz1 (Gao et al., 2018) and Gyp7 (as shown here) are only found within the endosomal system and not on the vacuole, Ypt7 activation and cycling seems to be largely confined to late endosomes. By enhancing the Ypt7 cycle, we have been able to trap Ypt7 at the late endosomes, which thereby greatly facilitate its examination by fluorescence microscopy. This has allowed us now to separate Vps21- and ESCRT-positive endosomes, and thus still immature MVBs, from Ypt7-positive late endosomes, which may include signaling endosomes. Moreover, this interpretation of a maturing MVB would also explain the persistence of a prevacuolar compartment proximal to the vacuole (Casler and Glick, 2020; Raymond et al., 1992; Prescianotto-Baschong and Riezman, 2002; Bryant et al., 1998; Gerrard et al., 2000; Singer and Riezman, 1990; Vida et al., 1990; Day et al., 2018; Griffith and Reggiori, 2009). Here, maturation of Vps21 to Ypt7 positive endosomes is paralleled by signaling via the TORC1 complex, which may delay fusion of MVBs. Likewise, recycling of proteins from MVBs via the retromer and other retrograde transport systems as well as a change in lipid composition such as PI(3)P or PI(3,5)P_2 may delay the fusion of late MVBs (Laidlaw et al., 2022; Suzuki et al., 2021; Chi et al., 2014; Liu et al., 2012). It is also likely that even this late Ypt7-positive MVB population is not homogenous as endocytic transport of selected cargos to the vacuole occurs rather efficiently (Day et al., 2018; Casler and Glick, 2020). However, we do not yet understand how this transition is controlled precisely. We expect that both the Ypt7 GEF and GAP, i.e., Mon1-Ccz1 and Gyp7, are regulated in their activity as both Mon1-Ccz1 (Langemeyer et al., 2020) and Gyp7 (as shown here) also colocalize with Vps21-positive early endosomal compartments.

Our data further suggest that Gyp7 also regulates TORC1 function via Ypt7 as cells with more Ypt7-positive structures due to Gyp7 overexpression have higher endosomal TORC1 activity, whereas *gyp7*Δ cells have reduced vacuolar TORC1 activity. In this regard, our findings agree

with observations in mammalian cells, in which the inactivation of TBC1D5 resulted in hyperactive Rab7, a mixing of Rab5 and Rab7 compartments and a strong defect in mTORC1 signaling (Kvainickas et al., 2019). Furthermore, enhanced endosomal TORC1 signaling in Gyp7 overexpression mutants suggests that the identity and possible fusion of signaling endosomes with the vacuole is tightly regulated. This may occur by phosphorylation events like the one of the Fab1 complex (Chen et al., 2021). Other possible targets are the Mon1-Ccz1 complex and Gyp7, whose activities clearly change signaling and late endosome biogenesis (Borchers et al., 2023) (this study). Likewise, HOPS complex activity might also be regulated. We also believe that signaling endosomes form after ESCRTs finished the formation of intraluminal vesicles. This could explain why several *VPS* mutants, including belonging to Class E, have a TORC1 signaling defect (Gao et al., 2022; Kingsbury et al., 2014). Finally, it is possible that Ypt7 effectors like retromer, Ivy1 and the HOPS complex, compete for the available Ypt7-pool. Further analysis of Gyp7 as a key regulator will be required to clarify how Ypt7 function and thus signaling at the late endosome is controlled.

Material & Methods

Strains and plasmids

Strains used in this study are listed in Table S1. A PCR- and homologous recombination-based approach with corresponding primers and templates was used to delete or endogenously tag genes (Janke et al., 2004). Plasmids used in this study are listed in Table S2.

Endogenous mutagenesis by CRISPR/Cas9

CRISPR/Cas9 was used to generate genomic point mutations in yeast strains (Generoso et al., 2016). Therefore, a Cas9-containing plasmid was built with a specific gRNA through the Gibson assembly strategy. The plasmid was transformed together with the corresponding homology directed repair fragment (HDR) (Table S2). Cells were recovered in YPD at 30°C for 2 h and then plated on the corresponding selection plate. Positive clones were selected by sequencing.

Expression and purification of proteins from *Escherichia coli*

GST-TEV-Ypt7, Ypt7-His_6, His_6-TEV-Gyp7, His_6-Sumo-Gyp7 TBC, Gyp1-46-His_6 and the prenylation machinery, Mrs6-His6, GST-PreSc-GDI and pCDF-DUET-Bet4 His_6-TEV-Bet2, were expressed in *Escherichia coli* BL21 DE3 (Rosetta) cells. Cells were grown in the presence of the corresponding antibiotics at 37°C in Luria Broth (LB) medium until an OD_{600} = 0.6 before protein expression was induced by the addition of 0.25 mM (or 0.5 mM for His_6-TEV-Gyp7, His_6-Sumo-Gyp7 TBC and Gyp1-46-His_6) isopropyl-β-d-thiogalactoside (IPTG). After 16-18 h

of protein expression at 16°C, cells were harvested by centrifugation at 4,000 *g*, 4°C for 10 min. Cells were resuspended in buffer containing 50 mM HEPES, pH 7.5, 150 mM NaCl, 1 mM $MgCl_2$, 1 mM DTT (GST-TEV-Ypt7, Ypt7-His_6, , Gyp1-46-His_6) or buffer containing 20 mM Na_2HPO_4/NaH_2PO_4, pH 7.4, 500 mM NaCl (His_6-TEV-Gyp7, His_6-Sumo-Gyp7 TBC). Cells expressing GST-PreSc-GDI were resuspended in PBS containing 5 mM β-mercaptoethanol (β-MeOH), while cells expressing the other components of the prenylation machinery were resuspended in buffer containing 50 mM Tris-HCl, pH 8.0, 300 mM NaCl, 2 mM β-MeOH. During lysis, buffers were supplemented with 1 mM phenylmethylsulfonyl fluoride (PMSF) and 0.1x protease inhibitor cocktail (PIC; a 20x stock solution contained 2 µg/ml Leupeptin, 10 mM 1,10-Phenanthroline, 10µg/ml Pepstatin A and 2 mM Pefablock). Cell lysis was performed in a Microfluidizer (Microfluidics, Inc.), and the cell lysate was cleared during centrifugation at 40,000 *g*, 4°C for 30 min. The cleared lysate was incubated with nickel-nitriloacetic acid (Ni-NTA) agarose (Qiagen) for purification of His-fusion proteins (Ypt7-His_6, His_6-TEV-Gyp7, His_6-Sumo-Gyp7 TBC, Mrs6-His_6 and Bet4 His_6-TEV-Bet2) or with glutathione sepharose (GSH) fast flow beads (GE Healthcare) for GST-fusion proteins (GST-TEV-Ypt7, GST-PreSc-GDI). After incubation for 2 h, 4°C on a turning wheel and extensive washing of the beads, His-fusion proteins were eluted from the beads with the respective buffer containing 300 mM imidazole. GST-fusion proteins were cleaved from the beads during incubation with TEV protease (GST-TEV-Ypt7) or PreScission protease (GST-PreSc-GDI) for 2 h at 16°C on a turning wheel. His_6-TEV-Ypt7, His_6-Mrs6 and Bet4 His_6-TEV-Bet2 were dialyzed into buffer containing 50 mM HEPES-NaOH, pH 7.4, 150 mM NaCl, 1.5 mM $MgCl_2$ and 1 mM DTT overnight with one buffer exchange. The buffer of purified GDI, His_6-TEV-Gyp7, His_6-Sumo-Gyp7 TBC and Gyp1-46-His_6 was exchanged using a PD-10 desalting column (GE Healthcare). Proteins were snap frozen and stored in aliquots at -80°C.

In vitro prenylation of Rab GTPases

Prenylated Rab-GDI complexes were generated as previously described (Langemeyer et al., 2020). Rab GTPases were pre-loaded with GDP (Sigma Aldrich, Germany) and then prenylated in buffer containing 50 mM HEPES-NaOH, pH 7.4, 150 mM NaCl, 1.5 mM $MgCl_2$ and 1 mM DTT.

Preparation of liposomes

Lipids were purchased from Avanti Polar Lipids, Inc., except for ergosterol (Sigma Aldrich, Germany) and 1,1'-Dioctadecyl-3,3,3',3'-Tetramethylindodicarbocyanine (DiD; Life Technologies). Liposomes composed of the vacuolar mimicking lipid mix (Zick and Wickner, 2014b) or containing 81.5 mol % dilinoleoyl phosphatidylcholine (DLPC 18:2 18:2), 18 mol % dilinoleoyl phosphatidylethanolamine (DLPE 18:2 18:2) and 0.5 mol % DiD were prepared. The vacuolar mimicking lipid mix contained 47.1 mol % dilinoleoyl phosphatidylcholine (DLPC 18:2

18:2), 18 mol % dilinoleoyl phosphatidylethanolamine (DLPE 18:2 18:2), 18 mol % soy phosphatidylinositol (PI), 1 mol % dipalmitoyl phosphatidylinositol-3-phosphate (PI(3)P diC16), 4.4 mol % dilinoleoyl phosphatidylserine (DLPS 18:2 18:2), 2 mol % dilinoleoyl phosphatidic acid (DLPA 18:2 18:2), 8 mol % ergosterol, 1 mol % diacylglycerol (DAG 16:0 16:0) and 0.5 mol % DiD. Where indicated, liposomes contained 3 mol % dioleoyl [(N-(5-amino-1-carboxypentyl)iminodiacetic acid)succinyl] (DOGS NTA 18:1 18:1) and 3 mol % less DLPC. Lipid films were evaporated and either dissolved in buffer containing 50 mM HEPES-NaOH, pH 7.4, 150 mM NaCl, and 1.5 mM $MgCl_2$ (membrane association assay) or 50 mM HEPES-NaOH, pH 7.4, 150 mM NaCl (HPLC-based GTPase activity assay) or HEPES-NaOH, pH 7.4, 150 mM KOAc, and 2 mM $MgCl_2$ (GDI extraction assay). After five cycles of thawing and freezing in liquid nitrogen, liposomes were extruded to 100 nm using a hand extruder and polycarbonate filters (Avanti Polar Lipids, Inc.).

Membrane association assay

Membrane association of GTPase activating proteins was analyzed by incubation of 715 µM liposomes with 715 nM protein for 10 or, where indicated, 0 min at 27°C, followed by centrifugation for 45 min, 100,000 *g* at 4°C. Reactions were filled up with buffer containing 50 mM HEPES-NaOH, pH 7.4, 150 mM NaCl, and 1.5 mM $MgCl_2$ to a volume of 80 µl. Prior to incubation, proteins were centrifuged for 1 h, 100,000 *g* at 4°C. Pelleted liposomes were separated from the supernatant. Proteins in the supernatant were precipitated by addition of 13% trichloro acetic acid. Upon wash with 100 % ice-cold acetone, supernatant and pellet fractions were analyzed by SDS-PAGE. Band intensity was measured by Fiji (NIH, Bethesda, MD). To determine the percentage of GAPs bound to membranes, the intensity signal of GAP in the pellet was normalized to the intensity signal in the corresponding supernatant.

GDI extraction assay

The GTPase activities of GAPs on membranes were analyzed in a GDI extraction assay according to Thomas et al., 2021 with modifications. For activation of prenylated Ypt7 on membranes, 0.6 µM Ypt7-GDI complex was incubated with 250 µM liposomes in the presence of 125 µM GTP (Sigmal Aldrich, Germany) and 3.75 mM EDTA, pH 8.0 for 30 min at 30°C. Nucleotide loading was stopped by addition of 7.5 mM $MgCl_2$. 3.75 nM Gyp7 was added to the reaction, which was filled up to a volume of 80 µl with buffer containing 20 mM HEPES-NaOH, pH 7.4, 150 mM NaCl, 1.5 mM $MgCl_2$. Where indicated, titration of the respective GAP (Gyp7, Gyp7-TBC, Gyp1-46) was performed, or reaction buffer was added instead. Furthermore, 6 µM Gdi1 was added to the reactions, where indicated. Reactions were incubated for 10 min at 27°C or for the indicated time points. Liposomes with bound protein were separated from unbound proteins using discontinuous density gradient centrifugation. For this, 100 µl of 2.5 M sucrose dissolved in HKM buffer (20 mM HEPES-NaOH, pH 7.4, 150 mM KOAc and 2 mM

$MgCl_2$) was added to the reactions ("input"). 150 µl of the reactions were transferred to polycarbonate centrifuge tubes (Beckman coulter, cat# 343778), overlayed with 200 µl of 0.75 M sucrose dissolved in HKM buffer, followed by 50 µl HKM buffer. Centrifugation was done at 285,000 *g*, 20°C for 25 min. Liposomes were collected from the top fraction of the sucrose gradient, and proteins were then precipitated by addition of 13 % trichloro acetic acid, followed by wash with 100 % ice-cold acetone. Samples were analyzed by SDS-PAGE and Western blotting using an antibody against Ypt7. Band intensities of the float and input fractions were measured with Fiji (NIH, Bethesda, MD). To quantify the percentage of Ypt7 bound to liposomes, the intensity signal of floated Ypt7 was compared to the intensity signal of the respective input and then normalized to the average value of the reaction containing no GAP.

HPLC-based GTPase activity assay

A HPLC-based GTPase activity assay was used to compare the GTPase activities of GAPs towards soluble Ypt7 in the presence and absence of membranes (Eberth and Ahmadian, 2009; Araki et al., 2021). 5 µM Ypt7 was incubated with 5 µM GAP and 50 µM GTP in the presence of 1 mM DTT, 20 mM EDTA, pH 8.0, and 5 mM $MgCl_2$ in reaction buffer (50 mM HEPES-NaOH pH 7.4, 150 mM NaCl). Where indicated, reactions contained 1 mM liposomes of the VML composition or PC/PE liposomes. Control reactions contained either no Ypt7, no GAP or neither Ypt7 nor GAP. All reactions had a volume of 160 µl and were incubated at 25°C. 30 µl samples of each reaction were snap frozen after 0 and 300 min reaction time and, where indicated, after 10, 60 and 180 min. All samples were boiled at 95°C for 5 min, and then 10 % perchloric acid was added. Samples were spun for 30 min, 20,500 *g* at 4°C. Supernatants were transferred and 20 µl were analyzed with an Agilent1260 Infinity HPLC system equipped with an autoloader and a diode array detector (190-640 nm). Samples were separated on a Nucleodur C18 Pyramid column (5 µm, 125 × 4 mm, Macherey-Nagel) by applying ion pair conditions using a gradient from buffer X (33.72 mM K_2HPO_4, 66.28 mM KH_2PO_4, pH 6.5; 10 mM tetrabutylammonium bromide) to buffer Y (1:1 buffer X:acetonitrile). The absorbance at 254 nm was monitored, GDP and GTP were eluted after 7.3 and 10.9 min, respectively, and the peak areas were measured with OpenChrom. For each time point, the percentage of GDP and GTP in each sample was determined. The percentage of GTP left at each time point was normalized to the respective percentage of GTP at t = 0 min.

Fluorescence microscopy and image analysis

Yeast cells were grown in synthetic complete media (SDC+all) overnight at 30°C. In the morning, cells were diluted to an OD_{600} = 0.15 and grown to logarithmic phase at 30°C. 1 OD_{600} equivalent of cells was pelleted. Vacuoles were stained with 7-amino-4-chloromethylcoumarin (CMAC) or FM4-64 (Thermo Fisher Scientific). For CMAC staining of the vacuolar lumen, cells were incubated with 0.1 mM CMAC for 15 min at 30°C, followed by washing with media twice.

For staining of the vacuolar membrane with the lipophilic dye FM4-64, pelleted cells were incubated with 30 µM FM4-64 for 20 min at 30°C. Cells were washed with media twice, and then incubated for 30 min at 30°C, and washed with media once. When mitochondrial DNA was stained, cells were incubated with 1 mg/ml 4′,6-diamidino-2-phenylindole (DAPI) (Thermo Fisher Scientific) for 15 min, followed by washing with media twice.

To monitor the uptake of the methionine transporter Mup1-GFP, cells were grown overnight in SDC media lacking methionine (SDC-MET) and diluted in SDC-MET media in the next morning. Cells of the logarithmic growth phase were either directly imaged or washed in SDC+all media twice, prior to incubation in SDC+all media for indicated time points. For induction of starvation, cells grown in SDC+all media until logarithmic phase were first washed with synthetic minimal medium lacking nitrogen (SD-N), and then incubated in SD-N for 1 or 2 h.

All cells were imaged at a DeltaVision Elite System, an Olympus IX-71 inverted microscope equipped with a 100x NA 1.49 objective, a sCMOS camera (PCO) and an InsightSSI illumination system, 4′,6-diamidino-2-phenylindole, GFP, mCherry, and Cy5 filters. Cells were imaged in z-stacks with 0.4 µM spacing. Deconvolution of images was performed using SOftWoRx software (Applied Precision). All images were processed in Fiji (NIH, Bethesda, MD) and one representative z-slice is depicted for each image. Quantification details are described in the corresponding figure legends.

Growth test

Yeast cells were grown overnight in YPD media at 30°C. In the morning, cells were diluted to OD_{600} = 0.1 and grown to logarithmic phase at 30°C. Cells were diluted to OD_{600} = 0.25 in YPD, spotted onto plates in serial dilutions (1:10), and incubated at indicated temperatures. Control and selection plates were used. Growth was monitored for several days.

ET/VT assay to measure TORC1 activities

The assays were carried out as previously described (Gao et al., 2022). Mutant strains and the respective wild-type were transformed with plasmids harboring either the ET reporter (FYVE-GFP-Sch9$^{C\text{-}term}$, p3027) or the VT reporter (Sch9$^{C\text{-}term}$-GFP-Pho8$^{N\text{-}term}$, p2976). Cells (10 ml) were grown at 30°C in SDC+all until mid-log phase and treated with TCA (trichloroacetic acid) at a final concentration of 6 %. Cells were isolated by centrifugation and the pellet was washed with cold acetone and dried in a speed-vac. The pellet was resuspended in lysis buffer (50 mM Tris-HCl, pH 7.5, 5 mM EDTA, 6 M urea, 1 % SDS), the amount being proportional to the OD_{600} of the original cell culture. To extract proteins, cells were lysed by agitation in a Precellys machine after addition of glass beads. After the addition of 2x Laemmli buffer (350 mM Tris-HCl, pH 6.8, 30 % glycerol, 600 mM DTT, 10 % SDS, BBF), the mix was boiled at 98°C for 5

min. The analysis was carried out by SDS-PAGE using phosphospecific rabbit anti-Sch9-pThr737 (custom made) and mouse anti-GFP (Roche, cat# 11814460001) antibodies. Band intensities were quantified using ImageJ software.

Immuno-electron microscopy

SEY6210 *ypt7*Δ pRS406-Ypt7pr-mNeon-4x(GGSG)-Ypt7-Ypt7term and SEY6210 *ypt7*Δ pRS406-Ypt7pr-mNeon-4x(GGSG)-Ypt7-Ypt7term Mon1$^{\Delta 100}$ *TEF1*pr-*GYP7* strains were grown in YPD to exponential phase and fixed, embedded in 12 % gelatin and cryo-sectioned as previously described in Griffith et al. (2008). 70 nm ultrathin cryo-sections were stained with with 2 % uranyloxalacetate, pH 7, for 5 min, and methyl-cellulose/uranyl acetate, pH 4, for additional 5 min. Cell sections were imaged using a Jeol-1400 transmission electron microscope equipped with a digital camera.

The strain expressing GFP-Ypt7 from the *TEF1* promoter was grown to an exponential phase before being processed for immunogold labeling of cryosections as previously described (Griffith et al., 2008). Cryo-sections were labelled with a polyclonal anti-GFP antibody (Abcam, cat# ab290-50) and viewed in a Jeol 1200 transmission electron microscope (Jeol, Tokyo, Japan), and images were recorded on Kodak 4489 sheet films (Eastman Kodak, Rochester, NY).

Acknowledgements

We thank Angela Perz for expert technical assistance and Clara Taetz and Kevin Tanzusch for experimental support. This work was supported by the grants of the Deutsche Forschungsgemeinschaft (DFG) to C.U. (SFB 944, P11; SFB 1557, P14), and to D.K. (SFB 944, P17; SFB 1557, P10), and the Swiss National Science Foundation (310030_184671) to C.D.V. F.R. is supported by Open Competition ENW-KLEIN (OCENW.KLEIN.118), SNSF Sinergia (CRSII5_189952) and Novo Nordisk Foundation (0066384) grants.

Author contributions

CU and LL conceived the project together with NF. NF performed all biochemistry and cell biology experiments with support of ACB. RN and CdV conducted and interpreted the TORC1 activity assays. MM, JG and FR conducted and interpreted the IEM analysis. EH, RR and DK analyzed the *in vitro* GAP assay together with NF. NF, CU and LL wrote the manuscript with contributions of all authors.

References

730 Albert, S., E. Will, and D. Gallwitz. 1999. Identification of the catalytic domains and their functionally
731 critical arginine residues of two yeast GTPase-activating proteins specific for Ypt/Rab transport
732 GTPases. *The EMBO journal*. 18:5216–5225.

733 Araki, M., K. Yoshimoto, M. Ohta, T. Katada, and K. Kontani. 2021. Development of a versatile
734 HPLC-based method to evaluate the activation status of small GTPases. *J Biol Chem*. 297:101428.
735 doi:10.1016/j.jbc.2021.101428.

736 Arlt, H., K. Auffarth, R. Kurre, D. Lisse, J. Piehler, and C. Ungermann. 2015. Spatiotemporal
737 dynamics of membrane remodeling and fusion proteins during endocytic transport. *Mol Biol Cell*.
738 26:1357–1370. doi:10.1091/mbc.e14-08-1318.

739 Babst, M., B. Wendland, E.J. Estepa, and S.D. Emr. 1998. The Vps4p AAA ATPase regulates
740 membrane association of a Vps protein complex required for normal endosome function. *The*
741 *EMBO journal*. 17:2982–2993. doi:10.1093/emboj/17.11.2982.

742 Balderhaar, H.J. kleine, H. Arlt, C. Ostrowicz, C. Bröcker, F. Sündermann, R. Brandt, M. Babst, and
743 C. Ungermann. 2010. The Rab GTPase Ypt7 is linked to retromer-mediated receptor recycling and
744 fusion at the yeast late endosome. *J Cell Sci*. 123:4085–4094. doi:10.1242/jcs.071977.

745 Barr, F.A. 2013. Rab GTPases and membrane identity: Causal or inconsequential? *J Cell Biol*.
746 202:191–199. doi:10.1083/jcb.201306010.

747 Bezeljak, U., H. Loya, B. Kaczmarek, T.E. Saunders, and M. Loose. 2020. Stochastic activation and
748 bistability in a Rab GTPase regulatory network. *Proc National Acad Sci*. 117:6540–6549.
749 doi:10.1073/pnas.1921027117.

750 Boomen, D.J.H. van den, A. Sienkiewicz, I. Berlin, M.L.M. Jongsma, D.M. van Elsland, J.P. Luzio,
751 J.J.C. Neefjes, and P.J. Lehner. 2020. A trimeric Rab7 GEF controls NPC1-dependent lysosomal
752 cholesterol export. *Nat Commun*. 11:5559. doi:10.1038/s41467-020-19032-0.

753 Borchers, A.-C., M. Janz, J.-H. Schäfer, A. Moeller, D. Kümmel, A. Paululat, C. Ungermann, and L.
754 Langemeyer. 2023. Regulatory sites in the Mon1-Ccz1 complex control Rab5 to Rab7 transition
755 and endosome maturation. *Proc. Natl. Acad. Sci. United States Am.* 120:e2303750120.
756 doi:10.1073/pnas.2303750120.

757 Borchers, A.-C., L. Langemeyer, and C. Ungermann. 2021. Who's in control? Principles of Rab
758 GTPase activation in endolysosomal membrane trafficking and beyond. *J Cell Biol*.
759 220:e202105120. doi:10.1083/jcb.202105120.

760 Brett, C.L., and A.J. Merz. 2008. Osmotic regulation of Rab-mediated organelle docking. *Current*
761 *biology : CB*. 18:1072–1077. doi:10.1016/j.cub.2008.06.050.

762 Brett, C.L., R.L. Plemel, B.T. Lobingier, B.T. Lobinger, M. Vignali, S. Fields, and A.J. Merz. 2008.
763 Efficient termination of vacuolar Rab GTPase signaling requires coordinated action by a GAP and
764 a protein kinase. *J Cell Biology*. 182:1141–1151. doi:10.1083/jcb.200801001.

765 Bryant, N., R. Piper, S. Gerrard, and T. Stevens. 1998. Traffic into the prevacuolar/endosomal
766 compartment of Saccharomyces cerevisiae: a VPS45-dependent intracellular route and a VPS45-
767 independent, endocytic route. *Eur J Cell Biol*. 76:43–52.

768 Cabrera, M., M. Nordmann, A. Perz, D. Schmedt, A. Gerondopoulos, F. Barr, J. Piehler, S.
769 Engelbrecht-Vandré, and C. Ungermann. 2014. The Mon1–Ccz1 GEF activates the Rab7 GTPase

Ypt7 via a longin-fold–Rab interface and association with PI3P-positive membranes. *J Cell Sci*. 127:1043–1051. doi:10.1242/jcs.140921.

Cabrera, M., and C. Ungermann. 2013. Guanine Nucleotide Exchange Factors (GEFs) Have a Critical but Not Exclusive Role in Organelle Localization of Rab GTPases*. *J Biol Chem*. 288:28704–28712. doi:10.1074/jbc.m113.488213.

Casler, J.C., and B.S. Glick. 2020. A microscopy-based kinetic analysis of yeast vacuolar protein sorting. *Elife*. 9:e56844. doi:10.7554/elife.56844.

Cezanne, A., J. Lauer, A. Solomatina, I.F. Sbalzarini, and M. Zerial. 2020. A non-linear system patterns Rab5 GTPase on the membrane. *Elife*. 9:e54434. doi:10.7554/elife.54434.

Chen, Z., P.C. Malia, R. Hatakeyama, R. Nicastro, Z. Hu, M.-P. Péli-Gulli, J. Gao, T. Nishimura, E. Eskes, C.J. Stefan, J. Winderickx, J. Dengjel, C.D. Virgilio, and C. Ungermann. 2021. TORC1 Determines Fab1 Lipid Kinase Function at Signaling Endosomes and Vacuoles. *Curr Biol*. 31:297-309.e8. doi:10.1016/j.cub.2020.10.026.

Chi, R.J., J. Liu, M. West, J. Wang, G. Odorizzi, and C.G. Burd. 2014. Fission of SNX-BAR–coated endosomal retrograde transport carriers is promoted by the dynamin-related protein Vps1. *J Cell Biol*. 204:793–806. doi:10.1083/jcb.201309084.

Conte-Zerial, P. del, L. Brusch, J.C. Rink, C. Collinet, Y. Kalaidzidis, M. Zerial, and A. Deutsch. 2008. Membrane identity and GTPase cascades regulated by toggle and cut-out switches. *Molecular Systems Biology*. 4:206. doi:10.1038/msb.2008.45.

Cui, Y., Q. Zhao, C. Gao, Y. Ding, Y. Zeng, T. Ueda, A. Nakano, and L. Jiang. 2014. Activation of the Rab7 GTPase by the MON1-CCZ1 Complex Is Essential for PVC-to-Vacuole Trafficking and Plant Growth in Arabidopsis. *Plant Cell*. 26:2080–2097. doi:10.1105/tpc.114.123141.

Day, K.J., J.C. Casler, and B.S. Glick. 2018. Budding Yeast Has a Minimal Endomembrane System. *Developmental cell*. 44:56-72.e4. doi:10.1016/j.devcel.2017.12.014.

Dehnen, L., M. Janz, J.K. Verma, O.E. Psathaki, L. Langemeyer, F. Fröhlich, J.J. Heinisch, H. Meyer, C. Ungermann, and A. Paululat. 2020. A trimeric metazoan Rab7 GEF complex is crucial for endocytosis and scavenger function. *J Cell Sci*. 133:jcs247080. doi:10.1242/jcs.247080.

Eberth, A., and M.R. Ahmadian. 2009. In Vitro GEF and GAP Assays. *Curr Protoc Cell Biology*. 43:14.9.1-14.9.25. doi:10.1002/0471143030.cb1409s43.

Eitzen, G., E. Will, D. Gallwitz, A. Haas, and W. Wickner. 2000. Sequential action of two GTPases to promote vacuole docking and fusion. *The EMBO journal*. 19:6713–6720.

Fidler, D.R., S.E. Murphy, K. Courtis, P. Antonoudiou, R. El-Tohamy, J. Ient, and T.P. Levine. 2016. Using HHsearch to tackle proteins of unknown function: A pilot study with PH domains. *Traffic*. 17:1214–1226. doi:10.1111/tra.12432.

Frasa, M.A.M., F.C. Maximiano, K. Smolarczyk, R.E. Francis, M.E. Betson, E. Lozano, J. Goldenring, M.C. Seabra, A. Rak, M.R. Ahmadian, and V.M.M. Braga. 2010. Armus Is a Rac1 Effector that Inactivates Rab7 and Regulates E-Cadherin Degradation. *Curr Biol*. 20:198–208. doi:10.1016/j.cub.2009.12.053.

Gao, J., L. Langemeyer, D. Kümmel, F. Reggiori, and C. Ungermann. 2018. Molecular mechanism to target the endosomal Mon1-Ccz1 GEF complex to the pre-autophagosomal structure. *Elife*. 7:e31145. doi:10.7554/elife.31145.

Gao, J., R. Nicastro, M.-P. Péli-Gulli, S. Grziwa, Z. Chen, R. Kurre, J. Piehler, C.D. Virgilio, F. Fröhlich, and C. Ungermann. 2022. The HOPS tethering complex is required to maintain signaling endosome identity and TORC1 activity. *J Cell Biol*. 221:e202109084. doi:10.1083/jcb.202109084.

Gerondopoulos, A., L. Langemeyer, J.-R. Liang, A. Linford, and F.A. Barr. 2012. BLOC-3 Mutated in Hermansky-Pudlak Syndrome Is a Rab32/38 Guanine Nucleotide Exchange Factor. *Curr Biol*. 22:2135–2139. doi:10.1016/j.cub.2012.09.020.

Gerrard, S., N. Bryant, and T. Stevens. 2000. VPS21 controls entry of endocytosed and biosynthetic proteins into the yeast prevacuolar compartment. *Molecular biology of the cell*. 11:613–626.

Griffith, J., M. Mari, A. de Mazière, and F. Reggiori. 2008. A cryosectioning procedure for the ultrastructural analysis and the immunogold labelling of yeast Saccharomyces cerevisiae. 9:1060–1072. doi:10.1111/j.1600-0854.2008.00753.x.

Griffith, J., and F. Reggiori. 2009. Ultrastructural analysis of nanogold-labeled endocytic compartments of yeast Saccharomyces cerevisiae using a cryosectioning procedure. *The journal of histochemistry and cytochemistry : official journal of the Histochemistry Society*. 57:801–809. doi:10.1369/jhc.2009.952952.

Hatakeyama, R., M.-P. Péli-Gulli, Z. Hu, M. Jaquenoud, G.M.G. Osuna, A. Sardu, J. Dengjel, and C.D. Virgilio. 2019. Spatially Distinct Pools of TORC1 Balance Protein Homeostasis. *Mol Cell*. 73:325-338.e8. doi:10.1016/j.molcel.2018.10.040.

Hatakeyama, R., and C.D. Virgilio. 2019. A spatially and functionally distinct pool of TORC1 defines signaling endosomes in yeast. *Autophagy*. 15:915–916. doi:10.1080/15548627.2019.1580107.

Hegedűs, K., S. Takáts, A. Boda, A. Jipa, P. Nagy, K. Varga, A.L. Kovács, and G. Juhász. 2016. The Ccz1-Mon1-Rab7 module and Rab5 control distinct steps of autophagy. *Mol Biol Cell*. 27:3132–3142. doi:10.1091/mbc.e16-03-0205.

Herrmann, E., L. Langemeyer, K. Auffarth, C. Ungermann, and D. Kümmel. 2023. Targeting of the Mon1-Ccz1 Rab guanine nucleotide exchange factor to distinct organelles by a synergistic protein and lipid code. *J Biol Chem*. 299:102915. doi:10.1016/j.jbc.2023.102915.

Hutagalung, A.H., and P.J. Novick. 2011. Role of Rab GTPases in Membrane Traffic and Cell Physiology. *Physiological Reviews*. 91:119–149. doi:10.1152/physrev.00059.2009.

Janke, C., M.M. Magiera, N. Rathfelder, C. Taxis, S. Reber, H. Maekawa, A. Moreno-Borchart, G. Doenges, E. Schwob, E. Schiebel, and M. Knop. 2004. A versatile toolbox for PCR-based tagging of yeast genes: new fluorescent proteins, more markers and promoter substitution cassettes. *Yeast (Chichester, England)*. 21:947–962. doi:10.1002/yea.1142.

Jia, D., J.-S. Zhang, F. Li, J. Wang, Z. Deng, M.A. White, D.G. Osborne, C. Phillips-Krawczak, T.S. Gomez, H. Li, A. Singla, E. Burstein, D.D. Billadeau, and M.K. Rosen. 2016. Structural and mechanistic insights into regulation of the retromer coat by TBC1d5. *Nat Commun*. 7:13305. doi:10.1038/ncomms13305.

847 Jimenez-Orgaz, A., A. Kvainickas, H. Nägele, J. Denner, S. Eimer, J. Dengjel, and F. Steinberg. 2018.
848 Control of RAB7 activity and localization through the retromer-TBC1D5 complex enables RAB7-
849 dependent mitophagy. *The EMBO Journal*. 37:235–254. doi:10.15252/embj.201797128.

850 Kanno, E., K. Ishibashi, H. Kobayashi, T. Matsui, N. Ohbayashi, and M. Fukuda. 2010.
851 Comprehensive Screening for Novel Rab-Binding Proteins by GST Pull-Down Assay Using 60
852 Different Mammalian Rabs‡. *Traffic*. 11:491–507. doi:10.1111/j.1600-0854.2010.01038.x.

853 Kinchen, J.M., and K.S. Ravichandran. 2010. Identification of two evolutionarily conserved genes
854 regulating processing of engulfed apoptotic cells. *Nature*. 464:778–782. doi:10.1038/nature08853.

855 Kingsbury, J.M., N.D. Sen, T. Maeda, J. Heitman, and M.E. Cardenas. 2014. Endolysosomal
856 Membrane Trafficking Complexes Drive Nutrient-Dependent TORC1 Signaling to Control Cell
857 Growth in Saccharomyces cerevisiae. *Genetics*. 196:1077–1089. doi:10.1534/genetics.114.161646.

858 Kucharczyk, R., A.M. Kierzek, P.P. Slonimski, and J. Rytka. 2001. The Ccz1 protein interacts with
859 Ypt7 GTPase during fusion of multiple transport intermediates with the vacuole in S. cerevisiae. *J*
860 *Cell Sci*. 114:3137–45. doi:10.1242/jcs.114.17.3137.

861 Kvainickas, A., H. Nägele, W. Qi, L. Dokládal, A. Jimenez-Orgaz, L. Stehl, D. Gangurde, Q. Zhao, Z.
862 Hu, J. Dengjel, C.D. Virgilio, R. Baumeister, and F. Steinberg. 2019. Retromer and TBC1D5
863 maintain late endosomal RAB7 domains to enable amino acid–induced mTORC1 signaling. *J Cell*
864 *Biol*. 218:3019–3038. doi:10.1083/jcb.201812110.

865 Lachmann, J., F.A. Barr, and C. Ungermann. 2012. The Msb3/Gyp3 GAP controls the activity of the
866 Rab GTPases Vps21 and Ypt7 at endosomes and vacuoles. *Mol Biol Cell*. 23:2516–2526.
867 doi:10.1091/mbc.e11-12-1030.

868 Laidlaw, K.M.E., G. Calder, and C. MacDonald. 2022. Recycling of cell surface membrane proteins
869 from yeast endosomes is regulated by ubiquitinated Ist1. *J Cell Biol*. 221:e202109137.
870 doi:10.1083/jcb.202109137.

871 Langemeyer, L., A.-C. Borchers, E. Herrmann, N. Füllbrunn, Y. Han, A. Perz, K. Auffarth, D.
872 Kümmel, and C. Ungermann. 2020. A conserved and regulated mechanism drives endosomal Rab
873 transition. *Elife*. 9:e56090. doi:10.7554/elife.56090.

874 Li, Y., B. Li, L. Liu, H. Chen, H. Zhang, X. Zheng, and Z. Zhang. 2015. FgMon1, a guanine
875 nucleotide exchange factor of FgRab7, is important for vacuole fusion, autophagy and plant
876 infection in Fusarium graminearum. *Scientific Reports*. 1–13. doi:10.1038/srep18101.

877 Lin, C.H., J.A. MacGurn, T. Chu, C.J. Stefan, and S.D. Emr. 2008. Arrestin-Related Ubiquitin-Ligase
878 Adaptors Regulate Endocytosis and Protein Turnover at the Cell Surface. *Cell*. 135:714–725.
879 doi:10.1016/j.cell.2008.09.025.

880 Liu, T.-T., T.S. Gomez, B.K. Sackey, D.D. Billadeau, and C.G. Burd. 2012. Rab GTPase regulation of
881 retromer-mediated cargo export during endosome maturation. *Molecular biology of the cell*.
882 23:2505–2515. doi:10.1091/mbc.e11-11-0915.

883 Malia, P., J. Numrich, T. Nishimura, A.G. Montoro, C.J. Stefan, and C. Ungermann. 2018. Control of
884 vacuole membrane homeostasis by a resident PI-3,5-kinase inhibitor. *Proc National Acad Sci*.
885 115:201722517. doi:10.1073/pnas.1722517115.

886 Markgraf, D.F., F. Ahnert, H. Arlt, M. Mari, K. Peplowska, N. Epp, J. Griffith, F. Reggiori, and C.
887 Ungermann. 2009. The CORVET Subunit Vps8 Cooperates with the Rab5 Homolog Vps21 to

Induce Clustering of Late Endosomal Compartments. *Mol Biol Cell*. 20:5276–5289. doi:10.1091/mbc.e09-06-0521.

McNally, K.E., and P.J. Cullen. 2018. Endosomal Retrieval of Cargo: Retromer Is Not Alone. *Trends in cell biology*. 28:807–822. doi:10.1016/j.tcb.2018.06.005.

Müller, M.P., and R.S. Goody. 2018. Molecular control of Rab activity by GEFs, GAPs and GDI. *Small Gtpases*. 9:5–21. doi:10.1080/21541248.2016.1276999.

Nordmann, M., M. Cabrera, A. Perz, C. Bröcker, C. Ostrowicz, S. Engelbrecht-Vandré, and C. Ungermann. 2010. The Mon1-Ccz1 Complex Is the GEF of the Late Endosomal Rab7 Homolog Ypt7. *Curr Biol*. 20:1654–1659. doi:10.1016/j.cub.2010.08.002.

Numrich, J., M.-P. Péli-Gulli, H. Arlt, A. Sardu, J. Griffith, T. Levine, S. Engelbrecht-Vandré, F. Reggiori, C.D. Virgilio, and C. Ungermann. 2015. The I-BAR protein Ivy1 is an effector of the Rab7 GTPase Ypt7 involved in vacuole membrane homeostasis. *J Cell Sci*. 128:2278–2292. doi:10.1242/jcs.164905.

Pan, X., S. Eathiraj, M. Munson, and D. Lambright. 2006. TBC-domain GAPs for Rab GTPases accelerate GTP hydrolysis by a dual-finger mechanism. *Nature*. 442:303–306.

Peralta, E.R., B.C. Martin, and A.L. Edinger. 2010. Differential Effects of TBC1D15 and Mammalian Vps39 on Rab7 Activation State, Lysosomal Morphology, and Growth Factor Dependence. 285:16814–16821. doi:10.1074/jbc.m110.111633.

Popovic, D., and I. Dikic. 2014. TBC1D5 and the AP2 complex regulate ATG9 trafficking and initiation of autophagy. *EMBO reports*. 15:392–401. doi:10.1002/embr.201337995.

Poteryaev, D., S. Datta, K. Ackema, M. Zerial, and A. Spang. 2010. Identification of the switch in early-to-late endosome transition. *Cell*. 141:497–508. doi:10.1016/j.cell.2010.03.011.

Prescianotto-Baschong, C., and H. Riezman. 2002. Ordering of Compartments in the Yeast Endocytic Pathway. *Traffic*. 3:37–49. doi:10.1034/j.1600-0854.2002.30106.x.

Purushothaman, L.K., H. Arlt, A. Kuhlee, S. Raunser, and C. Ungermann. 2017. Retromer-driven membrane tubulation separates endosomal recycling from Rab7/Ypt7-dependent fusion. *Mol Biol Cell*. 28:783–791. doi:10.1091/mbc.e16-08-0582.

Raymond, C., I. Howald-Stevenson, C. Vater, and T. Stevens. 1992. Morphological classification of the yeast vacuolar protein sorting mutants: evidence for a prevacuolar compartment in class E vps mutants. *Molecular biology of the cell*. 3:1389–1402.

Rink, J., E. Ghigo, Y. Kalaidzidis, and M. Zerial. 2005. Rab Conversion as a Mechanism of Progression from Early to Late Endosomes. *Cell*. 122:735–749. doi:10.1016/j.cell.2005.06.043.

Shimamura, H., M. Nagano, K. Nakajima, J.Y. Toshima, and J. Toshima. 2019. Rab5-independent activation and function of yeast Rab7-like protein, Ypt7p, in the AP-3 pathway. *Plos One*. 14:e0210223. doi:10.1371/journal.pone.0210223.

Shvarev, D., J. Schoppe, C. König, A. Perz, N. Füllbrunn, S. Kiontke, L. Langemeyer, D. Januliene, K. Schnelle, D. Kümmel, F. Fröhlich, A. Moeller, and C. Ungermann. 2022. Structure of the HOPS tethering complex, a lysosomal membrane fusion machinery. *Elife*. 11:e80901. doi:10.7554/elife.80901.

Singer, B., and H. Riezman. 1990. Detection of an intermediate compartment involved in transport of alpha-factor from the plasma membrane to the vacuole in yeast. *J Cell Biology*. 110:1911–1922. doi:10.1083/jcb.110.6.1911.

Singh, M.K., F. Krüger, H. Beckmann, S. Brumm, J.E.M. Vermeer, T. Munnik, U. Mayer, Y.-D. Stierhof, C. Grefen, K. Schumacher, and G. Jürgens. 2014. Protein delivery to vacuole requires SAND protein-dependent Rab GTPase conversion for MVB-vacuole fusion. *Current biology : CB*. 24:1383–1389. doi:10.1016/j.cub.2014.05.005.

Stroupe, C. 2018. This Is the End: Regulation of Rab7 Nucleotide Binding in Endolysosomal Trafficking and Autophagy. *Frontiers Cell Dev Biology*. 6:129. doi:10.3389/fcell.2018.00129.

Suzuki, S.W., A. Oishi, N. Nikulin, J.R. Jorgensen, M.G. Baile, and S.D. Emr. 2021. A PX-BAR protein Mvp1/SNX8 and a dynamin-like GTPase Vps1 drive endosomal recycling. *Elife*. 10:e69883. doi:10.7554/elife.69883.

Thomas, L.L., C.M. Highland, and J.C. Fromme. 2021. Arf1 orchestrates Rab GTPase conversion at the trans-Golgi network. *Mol Biol Cell*. 32:1104–1120. doi:10.1091/mbc.e20-10-0664.

Vaites, L.P., J.A. Paulo, E.L. Huttlin, and J.W. Harper. 2018. Systematic Analysis of Human Cells Lacking ATG8 Proteins Uncovers Roles for GABARAPs and the CCZ1/MON1 Regulator C18orf8/RMC1 in Macroautophagic and Selective Autophagic Flux. *Molecular and cellular biology*. 38. doi:10.1128/mcb.00392-17.

Varlakhanova, N.V., B.A. Tornabene, and M.G.J. Ford. 2018. Ivy1 is a negative regulator of Gtr-dependent TORC1 activation. *J Cell Sci*. 131:jcs218305. doi:10.1242/jcs.218305.

Vida, T.A., T.R. Graham, and S.D. Emr. 1990. In vitro reconstitution of intercompartmental protein transport to the yeast vacuole. *J Cell Biology*. 111:2871–2884. doi:10.1083/jcb.111.6.2871.

Vietri, M., M. Radulovic, and H. Stenmark. 2020. The many functions of ESCRTs. *Nat Rev Mol Cell Bio*. 21:25–42. doi:10.1038/s41580-019-0177-4.

Vollmer, P., E. Will, D. Scheglmann, M. Strom, and D. Gallwitz. 1999. Primary structure and biochemical characterization of yeast GTPase- activating proteins with substrate preference for the transport GTPase Ypt7p. *European journal of biochemistry / FEBS*. 260:284–290.

Wickner, W., and J. Rizo. 2017. A cascade of multiple proteins and lipids catalyzes membrane fusion. *Molecular Biology of the Cell*. 28:707–711. doi:10.1091/mbc.e16-07-0517.

Zhang, X.-M., B. Walsh, C.A. Mitchell, and T. Rowe. 2005. TBC domain family, member 15 is a novel mammalian Rab GTPase-activating protein with substrate preference for Rab7. *Biochem Bioph Res Co*. 335:154–161. doi:10.1016/j.bbrc.2005.07.070.

Zick, M., and W.T. Wickner. 2014a. A distinct tethering step is vital for vacuole membrane fusion. *Elife*. 3:e03251. doi:10.7554/elife.03251.

Zick, M., and W.T. Wickner. 2014b. A distinct tethering step is vital for vacuole membrane fusion. *eLife*. 3:e03251. doi:10.7554/elife.03251.

Zurita-Martinez, S.A., R. Puria, X. Pan, J.D. Boeke, and M.E. Cardenas. 2007. Efficient Tor signaling requires a functional class C Vps protein complex in Saccharomyces cerevisiae. *Genetics*. 176:2139–2150. doi:10.1534/genetics.107.072835.

Figure legends

Figure 1. Gyp7 localization depends on a functional endosomal system (A) Overview of Ypt7 function in fusion and fission reactions at the vacuole. For details, see text. **(B)** Localization of endogenously expressed Gyp7 and Msb3. Gyp7 and Msb3 were C-terminally tagged with mNeonGreen in wild-type (wt) and *vps4Δ* cells. Vacuolar membranes were stained with FM4-64 (see Methods). Cells were imaged by fluorescence microscopy. Individual slices are shown. Arrows depict Gyp7 accumulations. Scale bar, 2 µm. **(C)** Localization of endosomal markers relative to Gyp7. Marker proteins mCherry-Vps21 and Vps35-2xmKate were co-expressed in *vps4Δ* cells encoding endogenous Gyp7-mNeonGreen. Vacuoles were stained with CMAC (see Methods). Cells were imaged by fluorescence microscopy. Individual slices are shown. Arrows depict representative colocalization. Scale bar, 2 µm. **(D)** Quantification of Gyp7 puncta colocalizing with endosomal markers in (C). Cells (n≥100) from three independent experiments were quantified in Fiji. Bar graphs represent the averages from three experiments and puncta represent the mean of each experiment. **(E)** Localization of Gyp7 in selected deletion mutants. Gyp7 was tagged with mNeonGreen in wild-type, *vps21Δ ypt52Δ*, *vps3Δ*, *vps45Δ* and *mvp1Δ* cells. Vacuolar membranes were stained with FM4-64. Cells were imaged by fluorescence microscopy and individual slices are shown. Scale bar, 2 µm. **(F)** Quantification of Gyp7 puncta per cell in (E) and Fig. S1A. Cells (n≥100) from three independent experiments were quantified in Fiji. Bar graphs represent the averages from three experiments and puncta represent the mean of each experiment. (P-value **<0.01, ***<0.001, using ANOVA one-way test).

Figure 2. Vacuolar localization of Gyp7 impairs vacuolar function. (A) Vacuole morphology upon galactose-induced overexpression of Gyp7. Gyp7 was expressed from the *GAL1* promoter. Wild-type cells and cells encoding *GAL1*pr-*GYP7* were grown in glucose- or galactose-containing media (see Methods). Vacuolar membranes were stained with FM4-64. Cells were imaged by fluorescence microscopy and individual slices are shown. Scale bar, 2 µm. **(B)** Quantification of the number of vacuoles per cell in (A). Cells were grouped into three different classes: 1-2 vacuoles, 3-4 vacuoles (not shown) and >5 vacuoles. Cells (n≥100) from three independent experiments were quantified in Fiji. Bar graphs represent the averages and error bars the SD from three experiments. (P-value ns, **<0.01, ***<0.001 using ANOVA one-way test). **(C)** Vacuole morphology of cells expressing Vps8- or Zrc1-Chromobody. Vps8 and Zrc1 were C-terminally tagged with a nanobody against GFP (CB). Vacuolar membranes were stained with FM4-64. Cells were imaged by fluorescence microscopy and individual slices are shown. Scale bar, 2 µm. **(D)** Vacuole morphology of cells with Gyp7 targeted to endosomes or

the vacuole. Vps8 and Zrc1 were C-terminally tagged with CB in cells expressing Gyp7-GFP. Where indicated, an Ypt7 fast cycling mutant ($Ypt7^{K127E}$) was expressed from an integrative plasmid. Vacuolar membranes were stained with FM4-64. Cells were imaged by fluorescence microscopy and individual slices are shown. Scale bar, 2 µm. **(E)** Quantification of the number of vacuoles per cell in (C) and (D). Cells were classified as in (B). Cells (n≥150) from three independent experiments were quantified in Fiji. Bar graphs represent the averages and error bars the SD from three experiments. (P-value *<0.05, **<0.01 and ***<0.001, using ANOVA one-way test). **(F)** Vacuole morphology of cells expressing $Gyp7^{R458K}$, the catalytic dead mutant of Gyp7. The mutation was introduced into cells expressing Gyp7-GFP. Where indicated, Vps8 and Zrc1 were C-terminally tagged with a chromobody (CB). Vacuolar membranes were stained with FM4-64. Cells were imaged by fluorescence microscopy and individual slices are shown. Scale bar, 2 µm. **(G)** Quantification of the number of vacuoles per cell in (F). Cells were classified as in (B). Cells (n≥130) from three independent experiments were quantified in Fiji. Bar graphs represent the averages and error bars the SD from three experiments. (P-value ns, using ANOVA one-way test).

Figure 3. Gyp7 is required for endosomal physiology and efficient endocytosis. (A) Growth assay on $ZnCl_2$-containing plates. Indicated yeast strains were grown to the same OD_{600} in YPD media and serial dilutions were spotted onto agar plates containing YPD or YPD supplemented with 4 mM $ZnCl_2$ (see Methods). Plates were incubated at 30°C for several days before imaging. Images are representative for three independent experiments. **(B)** Growth assay on Rapamycin-containing plates. Indicated yeast strains were spotted onto agar plates containing YPD or YPD supplemented with 50 ng/ml Rapamycin as in (A). Plates were incubated at 30°C for several days before imaging. Images are representative for three independent experiments. **(C)** Endocytosis of Mup1 in wild-type and *gyp7Δ* cells. Cells were grown to logarithmic phase in SDC-MET media, analyzed by fluorescence microscopy and then shifted to SDC+all media. Cells were imaged at indicated time points by fluorescence microscopy. Individual slices are shown. Scale bar, 2 µm. **(D)** Quantification of the vacuole to plasma membrane fluorescence intensity ratio of Mup1 in (C). The maximal fluorescence intensity of Mup1-GFP signal in the vacuolar lumen was divided by the maximal intensity of Mup1 at the plasma membrane. For each time point, cells (n≥100) from three independent experiments were quantified in Fiji. Bar graphs represent the averages and error bars the SD from three experiments. (P-value ns, **<0.01, ***<0.001, using two-sample t-test). **(E)** Quantification of Mup1-GFP puncta per cell in (C). For each time point, cells (n≥100) from three independent experiments were quantified in Fiji. Bar graphs represent the averages and error bars the SD from three experiments. (P-value ns, **<0.01, using two-sample t-test). **(F)** Vacuole morphology of wild-type and *gyp7Δ* cells in growth and starvation conditions. Cells were grown in SDC+all and then shifted to SD-N for 2 h, where indicated (see Methods). Cells

were imaged by fluorescence microscopy and individual slices are shown. Scale bar, 2 µm. **(G)** Quantification of the number of vacuoles per cell in (F) during growth. Cells were grouped into three different classes: 1-2 vacuoles, 3-4 vacuoles and >5 vacuoles. Cells (n≥150) from three independent experiments were quantified in Fiji. Bar graphs represent the averages from three experiments and puncta represent the mean of each experiment. (P-value ns, using ANOVA one-way test). **(H)** Quantification of the number of vacuoles per cell in (F) during nitrogen starvation. Cells were grouped as described in (G). Cells (n≥150) from three independent experiments were quantified in Fiji. Bar graphs represent the averages from three experiments and puncta represent the mean of each experiment. (P-value ns, using ANOVA one-way test).

Figure 4. Gyp7 requires a distinct membrane environment for efficient GAP activity. (A) Overview of the GDI extraction assay. 250 µM liposomes with VML composition are pre-loaded with 0.6 µM Ypt7-GDI complex in the presence of 3.75 mM EDTA and 125 µM GTP. The nucleotide binding is stabilized by addition of 7.5 mM $MgCl_2$. Incubation with the GAP Gyp7 triggers GTP hydrolysis. GDI extracts inactivated Ypt7 from liposomal membranes. Liposomes with bound Ypt7 are floated in a sucrose gradient and separated from unbound protein. Floated membrane fractions and inputs are analyzed by Western blotting (see Methods). **(B)** Ypt7 inactivation increases with the concentration of Gyp7. Assay was performed as in (A). Reactions were incubated with different amounts of Gyp7 for 1 h. Control reaction contained no Gyp7. 40 % of the float was analyzed together with 3 % input by Western blotting using an anti-Ypt7 antibody. **(C)** Quantification of bound Ypt7 to liposomes in (B). Band intensity of Ypt7 signal in float was measured in Fiji and compared to input. Reactions containing Gyp7 were normalized to the average value of the control reaction. Bar graphs represent the averages from three independent experiments and puncta represent the mean of each experiment. (P-value ns, *<0.05, **<0.01, using ANOVA one-way test). **(D)** Kinetics of Gyp7 activity towards Ypt7-GTP. Assay was performed as in (A). Reactions were incubated with 0.75 nM Gyp7 for different time points. Control reaction contained no Gyp7. 40 % of the float was analyzed together with 3 % input by Western blotting using an anti-Ypt7 antibody. **(E)** Quantification of bound Ypt7 to liposomes in (D). Quantification was performed as in (C). (P-value *<0.05, **<0.01, ***<0.001 using ANOVA one-way test). **(F)** Membrane association of Gyp7. 715 µM liposomes with VML composition were incubated with 715 nM Gyp7 for 10 min. Membranes were separated from supernatant by centrifugation at 100,000 g and both fractions were analyzed by SDS-PAGE and Coomassie staining. Control reaction contained no liposomes (see Methods). **(G)** Quantification of the relative Gyp7 amount in the pellet in (F). Band intensity of Gyp7 signal in the pellet was measured in Fiji and compared to Gyp7 signal in the supernatant. Bar graphs represent the averages from three independent experiments and puncta represent the mean of each experiment. (P-value *<0.05, using two-sample t-test). **(H)**

Comparison of Gyp7 activity on liposomes with VML composition and PC/PE liposomes. Assay was performed as in (A). 3.75 nM Gyp7 was added to reactions containing liposomes with VML composition or PC/PE liposomes for 10 min. Control reactions contained respective liposomes and no Gyp7. 40 % of the float was analyzed together with 3 % input by Western blotting using an anti-Ypt7 antibody. **(I)** Quantification of bound Ypt7 to liposomes in (H). Quantification was performed as in (C). Reactions containing Gyp7 were normalized to the average value of the respective control reaction (P-value *<0.05, **<0.01, using ANOVA one-way test). **(J)** Association of Gyp7 with liposomes of VML composition and PC/PE liposomes. 715 nM Gyp7 was incubated with 715 µM liposomes for 0 and 10 min. Membrane association was analyzed as in (F). **(K)** Quantification of the relative Gyp7 amount in the pellet in (J). Quantification was performed as in (G). (P-value ns, *<0.05, using ANOVA one-way test). **(L)** Comparison of Gyp1-46 activity on liposomes with VML composition and PC/PE liposomes. Assay was performed as in (A), except for the addition of Gyp1-46 instead of Gyp7 to reactions. Reactions were incubated with different amounts of Gyp1-46 for 10 min. Control reactions contained respective liposomes and no GAP. 40 % of the float was analyzed together with 3 % input by Western blotting using an anti-Ypt7 antibody. **(M)** Quantification of bound Ypt7 to liposomes in (L). Quantification was performed as in (C). Reactions containing Gyp1-46 were normalized to the average value of the respective control reaction (P-value *<0.05, using ANOVA one-way test).

Figure 5. Gyp7 is activated by a distinct membrane environment. (A) Membrane association of Gyp7 with DOGS-NTA containing liposomes. 715 nM Gyp7 was incubated with 715 µM liposomes (VML + DOGS-NTA, PC/PE + DOGS-NTA, PC/PE) for 10 min. Membranes were separated from supernatant by centrifugation at 100,000 g and both fractions were analyzed by SDS-PAGE and Coomassie staining. Control reaction contained no liposomes. **(B)** Quantification of the relative Gyp7 amount in the pellet in (A). Band intensity of Gyp7 signal in the pellet was measured in Fiji and compared to Gyp7 signal in the supernatant. Bar graphs represent the averages from three independent experiments and puncta represent the mean of each experiment. (P-value ns, **<0.01, ***<0.001, using ANOVA one-way test). **(C)** Comparison of Gyp7 activity on DOGS-NTA containing liposomes. 250 µM liposomes were pre-loaded with 0.6 µM Ypt7:GDI complex in the presence of 3.75 mM EDTA and 125 µM GTP. Nucleotide binding was stabilized by addition of 7.5 mM $MgCl_2$. Reactions were incubated with 3.75 µM Gyp7 for 10 min. Liposomes were floated in a sucrose gradient. Control reactions contained no Gyp7. 40 % of the float was analyzed together with 3 % input by Western blotting using an anti-Ypt7 antibody. **(D)** Quantification of bound Ypt7 to liposomes in (C). Band intensity of Ypt7 signal in float was measured in Fiji and compared to input. Reactions containing Gyp7 were normalized to the average value of the respective control reaction. Bar graphs represent the averages from three independent experiments and puncta represent the

mean of each experiment. (P-value ns, ***<0.001, using ANOVA one-way test). (**E)** AlphaFold2 structure prediction of Gyp7. The N-terminal PH domain is colored blue and the C-terminal TBC domain is colored cyan with the catalytic Arg (R458) and Glu (Q531) residues shown red in stick representation. A middle domain, which is modeled with low pLDDT confidence scores (Fig. S4A, B), is colored green. **(F)** Membrane association of the TBC domain compared to full-length Gyp7. Gyp7 and the TBC domain were incubated with liposomes of VML composition as in (A). Control reactions contained no liposomes. **(G)** Quantification of the relative amount of Gyp7 in the pellet in (F). Quantification performed as in (B). (P-value *<0.05 using ANOVA one-way test). **(H)** Comparison of Gyp7 and TBC domain activities on liposomes with VML composition. Assay was performed as in (C). Pre-loaded liposomes were incubated with different amounts of Gyp7 or the TBC domain for 10 min. **(I)** Quantification of bound Ypt7 to liposomes in (H). Quantification was performed as in (D). Reactions containing GAP were normalized to the average value of the control reaction. (P-value ns, *<0.05, using ANOVA one-way test). **(J)** Comparison of Gyp7 activity towards soluble Ypt7-GTP in solution and on membranes. 5 µM Ypt7 was incubated with 5 µM GAP and 50 µM GTP in the presence of 1 mM DTT, 20 mM EDTA and 5 mM $MgCl_2$. Where indicated, reactions contained 1 mM liposomes with VML composition or PC/PE liposomes. Control reactions contained no Ypt7, no GAP or neither Ypt7 nor GAP (see Fig. S4G). Reactions were stopped after 0, 10, 60, 180 and 300 min by snap freezing and boiling at 95 °C. Samples were applied to a HPLC system and the absorbance of GDP and GTP was monitored at 254 nm. Peaks were analyzed with OpenChrom and for each time point the percentage of GDP and GTP in the samples was determined. The percentage of GTP left at each time point was normalized to the respective percentage of GTP at t = 0 min. Normalized % GTP left plotted against the time in min. Bar graphs represent the averages and error bars the SD from three independent experiments. (P-value **<0.01, ***<0.001, using ANOVA one-way test).

Figure 6. Gyp7 and Mon1-Ccz1 shift Ypt7 from the vacuole to dot-like structures. (A) The localization of Ypt7 depends on the expression level or activity of Gyp7 and Mon1-Ccz1. Endogenous mNeon-Ypt7 was expressed from an integrative plasmid in *ypt7Δ* cells. Where indicated, 100 amino acids at the N-terminus of Mon1 were deleted ($Mon1^{\Delta 100}$). Gyp7 was either deleted or expressed from the *TEF1* promoter in mNeon-Ypt7 expressing cells with wild-type Mon1 or $Mon1^{\Delta 100}$. Vacuolar membranes were stained with FM4-64. Cells were imaged by fluorescence microscopy. Individual slices are shown. Arrows depict Ypt7 accumulations not proximal to the vacuole. Scale bar, 2 µm. **(B)** Quantification of the total number of Ypt7 puncta per cell, the percentage of distant Ypt7 puncta and the fluorescence intensity of Ypt7 puncta in (A). The number of distant Ypt7 puncta (not at the vacuole) was divided by the total number of Ypt7 puncta per cell. The maximum fluorescence intensity of mNeon-Ypt7 puncta was normalized to the maximum fluorescence intensity of mNeon-Ypt7 at the vacuolar

membrane. Cells (n≥100) from three independent experiments were quantified in Fiji. Bar graphs represent the averages from three experiments and puncta represent the mean of each experiment. (P-value ns, *<0.05, **<0.01, ***<0.001, using ANOVA one-way test). **(C)** Localization of Gyp7 relative to Ypt7 and Mon1-Ccz1. Gyp7 was C-terminally tagged with 2xmKate in the Mon1^{100} strain, in *TEF1*pr-*GYP7* or wild-type cells encoding endogenous Ccz1-mNeon (top) or mNeon-Ypt7 (bottom). Vacuoles were stained with CMAC. Cells were imaged by fluorescence microscopy. Individual slices are shown. Arrows depict representative colocalization. Scale bar, 2 µm. **(D)** Quantification of Gyp7 puncta colocalizing with Ccz1 puncta in (C). Cells (n≥100) from three independent experiments were quantified in Fiji. Bar graphs represent the averages from three experiments and puncta represent the mean of each experiment. (P-value ns, ***<0.001, using ANOVA one-way test). **(E)** Quantification of Gyp7 puncta colocalizing with Ypt7 puncta in (C). Cells (n≥100) from three independent experiments were quantified in Fiji. Bar graphs represent the averages from three experiments and puncta represent the mean of each experiment. (P-value ns, using ANOVA one-way test).

Figure 7. Ypt7-positive puncta correspond to signaling endosomes. (A) Localization of mNeon-Ypt7 puncta relative to the endosomal marker Ivy1. Ivy1-mKate was expressed in *TEF1*pr-*GYP7* or wild-type cells encoding endogenous mNeon-Ypt7. Vacuoles were stained with CMAC. Cells were imaged by fluorescence microscopy. Individual slices are shown. Arrows depict representative colocalization. Scale bar, 2 µm. **(B)** Quantification of Ypt7 colocalizing with endosomal markers in (A) and Fig. S6A. Cells (n≥100) from three independent experiments were quantified in Fiji. Bar graphs represent the averages and error bars the SD from the three experiments. (P-value ns, ***<0.001, using two-sample t-test). **(C)** Quantification of the number of Pep12 puncta per cell in Fig. S6B. Cells (n≥150) from three independent experiments were quantified in Fiji. Bar graphs represent the averages from three experiments and puncta represent the mean of each experiment. (P-value ***<0.001, using ANOVA one-way test). **(D)** Quantification of the percentage of distant Pep12 puncta in Fig. S6B. The number of distant Pep12 puncta (not at the vacuole) was divided by the total number of Pep12 puncta per cell. Cells (n≥150) from three independent experiments were quantified in Fiji. Bar graphs represent the averages from three experiments and puncta represent the mean of each experiment. (P-value ***<0.001, using ANOVA one-way test). **(E)** Quantification of the number of Tco89 puncta per cell in Fig. S6C. Cells (n≥150) from three independent experiments were quantified in Fiji. Bar graphs represent the averages from three experiments and puncta represent the mean of each experiment. (P-value ns, using two-sample t-test).

Figure 8. Enhanced Ypt7 cycling affects endocytic trafficking. (A) Localization of Cps1 in wild-type, *TEF1*pr-*VPS8 ADH*pr-*VPS21* and Mon1$^{\Delta100}$-Ccz1 *TEF1*pr-*GYP7* cells. Vacuolar membranes were stained with FM4-64. Cells were imaged by fluorescence microscopy.

Individual slices are shown. Arrows depict Cps1 accumulations next to the vacuole. Scale bar, 2 µm. **(B)** Quantification of the number of Cps1 puncta per cell in (A). Cells (n≥140) from three independent experiments were quantified in Fiji. Bar graphs represent the averages from three experiments and puncta represent the mean of each experiment. (P-value **<0.01, ***<0.001, using ANOVA one-way test). **(C)** Quantification of the percentage of cells with Cps1 accumulations in (A). The number of cells with Cps1 accumulations at the vacuole was divided by the total number of cells. Cells (n≥140) from three independent experiments were quantified in Fiji. Bar graphs represent the averages from three experiments and puncta represent the mean of each experiment. (P-value ***<0.001, using ANOVA one-way test). **(D)** Endocytosis of Mup1 in cells with altered expression or activity of Gyp7 and Mon1-Ccz1. Cells were grown to logarithmic phase in SDC-MET media, analyzed by fluorescence microscopy and then shifted to SDC+all media. Cells were imaged at indicated time points by fluorescence microscopy. Individual slices are shown. Scale bar, 2 µm. **(E)** Quantification of the number of puncta to plasma membrane fluorescence intensity of Mup1 ratio in (D). For each cell, the number of Mup1 puncta was divided by the maximum fluorescence intensity of Mup1-GFP signal at the plasma membrane. For each time point, cells (n≥100) from three independent experiments were quantified in Fiji. Bar graphs represent the averages and error bars the SD from three experiments. (P-value ns, *<0.05, ***<0.001, using ANOVA one-way test).

Figure 9. Ypt7 functions on mature endosomes. (A) Growth assay on Rapamycin-containing plates. Indicated yeast strains were grown to the same OD_{600} in YPD media and serial dilutions were spotted onto agar plates containing YPD or YPD supplemented with 70 ng/ml Rapamycin. Plates were incubated at 37°C for several days before imaging. Images are representative for three independent experiments. **(B)** Ypt7 accumulates in the Class E compartment. Endogenous mNeon-Ypt7 was expressed from an integrative plasmid in *ypt7Δ vps4Δ* cells. Where indicated, Gyp7 was expressed from the *TEF1* promoter. Vacuolar membranes were stained with FM4-64. Cells were imaged by fluorescence microscopy. Individual slices are shown. Arrows depict Ypt7 accumulations in the Class E compartment. Scale bar, 2 µm. **(C)** Electron microscopy analysis of cells expressing mNeon-Ypt7 in wild-type and Mon1$^{\Delta 100}$-Ccz1 *TEF1*pr-*GYP7* cells (see Methods). M, mitochondria; V, vacuole; asterisk, multivesicular body. Scale bars, 200 nm. **(D)** IEM analysis of cells expressing *TEF1*pr-*GFP-YPT7*. Ypt7 was detected by using anti-GFP antibodies and protein A-conjugated gold (see Methods). Asterisk, multivesicular body; V, vacuole. Scale bars, 200 nm. **(E)** Working model of Gyp7 function on MVBs. MVBs form with the help of ESCRTs on Vps21/Rab5-positive endosomes (left), which carry yet inactive Mon1-Ccz1. Maturation of endosomes includes recruitment of Gyp7 and loss of Rab5 and its effector CORVET. Some of these late endosomes also acquire TORC1 and the Fab1 complex, thus turn into signaling endosomes. This may affect Gyp7 and Mon1-Ccz1 activity and thus control the available Ypt7 pool.

February 27, 2024

RE: JCB Manuscript #202305038R-A

Prof. Christian Ungermann
Osnabrück University
Biology/Chemistry
Barbarastrasse 13
Osnabrück 49076
Germany

Dear Prof. Ungermann:

Thank you for submitting your revised manuscript entitled "The GTPase activating protein Gyp7 regulates the activity of the Rab7-like Ypt7 on late endosomes". We would be happy to publish your paper in JCB pending resolution of remaining minor concerns by reviewers, and final revisions necessary to meet our formatting guidelines (see details below).

To avoid unnecessary delays in the acceptance and publication of your paper, please read the following information carefully.

A. MANUSCRIPT ORGANIZATION AND FORMATTING:

Full guidelines are available on our Instructions for Authors page, http://jcb.rupress.org/submission-guidelines#revised. Submission of a paper that does not conform to JCB guidelines will delay the acceptance of your manuscript.

1) Text limits: Character count for Articles is < 40,000, not including spaces. Count includes abstract, introduction, results, discussion, and acknowledgments. Count does not include title page, figure legends, materials and methods, references, tables, or supplemental legends.

2) Figures limits: Articles may have up to 10 main figures and 5 supplemental figures/tables.
** Please combine supplemental figure panels into corresponding main figure panels, or eliminate supplemental data to reduce total supplemental figures to 5. If appropriate, an additional main figure may also be generated.

3) Figure formatting: Scale bars must be present on all microscopy images, including inset magnifications. Molecular weight or nucleic acid size markers must be included on all gel electrophoresis. Please avoid pairing red and green for images and graphs to ensure legibility for color-blind readers. If red and green are paired for images, please ensure that the particular red and green hues used in micrographs are distinctive with any of the colorblind types. If not, please modify colors accordingly or provide separate images of the individual channels.
** Please include scale bars on Figure 9B and S1A.
** Please add molecular weight markers to Fig S7A.

4) Statistical analysis: Error bars on graphic representations of numerical data must be clearly described in the figure legend. The number of independent data points (n) represented in a graph must be indicated in the legend. Statistical methods should be explained in full in the materials and methods. For figures presenting pooled data the statistical measure should be defined in the figure legends. Please also be sure to indicate the statistical tests used in each of your experiments (either in the figure legend itself or in a separate methods section) as well as the parameters of the test (for example, if you ran a t-test, please indicate if it was one- or two-sided, etc.). Also, if you used parametric tests, please indicate if the data distribution was tested for normality (and if so, how). If not, you must state something to the effect that "Data distribution was assumed to be normal but this was not formally tested."

5) Abstract and title: The abstract should be no longer than 160 words and should communicate the significance of the paper for a general audience. The title should be less than 100 characters including spaces. Make the title concise but accessible to a general readership.
** We recommend changing the title to something slightly shorter: "The GTPase activating protein Gyp7 regulates Rab7/Ypt7 activity on late endosomes"

6) Materials and methods: Should be comprehensive and not simply reference a previous publication for details on how an experiment was performed. Please provide full descriptions in the text for readers who may not have access to referenced manuscripts. We also provide a report from SciScore and an associate score, which we encourage you to use as a means of evaluating and improving the methods section.
** Please provide full details for in vitro prenylation of Rab GTPases and immune-electron microscopy.

7) Please be sure to provide the sequences for all of your primers/oligos and RNAi constructs in the materials and methods. You must also indicate in the methods the source, species, and catalog numbers (where appropriate) for all of your antibodies. Please also indicate the acquisition and quantification methods for immunoblotting/western blots.

8) Microscope image acquisition: The following information must be provided about the acquisition and processing of images:
a. Make and model of microscope
b. Type, magnification, and numerical aperture of the objective lenses
c. Temperature
d. Imaging medium
e. Fluorochromes
f. Camera make and model
g. Acquisition software
h. Any software used for image processing subsequent to data acquisition. Please include details and types of operations involved (e.g., type of deconvolution, 3D reconstitutions, surface or volume rendering, gamma adjustments, etc.).

9) References: There is no limit to the number of references cited in a manuscript. References should be cited parenthetically in the text by author and year of publication. Abbreviate the names of journals according to PubMed.

10) Supplemental materials: There are strict limits on the allowable amount of supplemental data. Articles may have up to 5 supplemental figures. Please also note that tables, like figures, should be provided as individual, editable files. A summary of all supplemental material should appear at the end of the Materials and methods section.

11) eTOC summary: A ~40-50-word summary that describes the context and significance of the findings for a general readership should be included on the title page. The statement should be written in the present tense and refer to the work in the third person.

12) Conflict of interest statement: JCB requires inclusion of a statement in the acknowledgements regarding competing financial interests. If no competing financial interests exist, please include the following statement: "The authors declare no competing financial interests." If competing interests are declared, please follow your statement of these competing interests with the following statement: "The authors declare no further competing financial interests."

13) ORCID IDs: ORCID IDs are unique identifiers allowing researchers to create a record of their various scholarly contributions in a single place. At resubmission of your final files, please provide an ORCID ID for all authors.

14) A separate author contribution section following the Acknowledgments. All authors should be mentioned and designated by their full names. We encourage use of the CRediT nomenclature.

15) A data availability statement is required for all research article submissions. The statement should address all data underlying the research presented in the manuscript. Please visit the JCB instructions for authors for guidelines and examples of statements at (https://rupress.org/jcb/pages/editorial-policies#data-availability-statement).

Please note that JCB requires authors to submit Source Data used to generate figures containing gels and Western blots with all revised manuscripts. This Source Data consists of fully uncropped and unprocessed images for each gel/blot displayed in the main and supplemental figures. Since your paper includes cropped gel and/or blot images, please be sure to provide one Source Data file for each figure that contains gels and/or blots along with your revised manuscript files. File names for Source Data figures should be alphanumeric without any spaces or special characters (i.e., SourceDataF#, where F# refers to the associated main figure number or SourceDataFS# for those associated with Supplementary figures). The lanes of the gels/blots should be labeled as they are in the associated figure, the place where cropping was applied should be marked (with a box), and molecular weight/size standards should be labeled wherever possible. Source Data files will be directly linked to specific figures in the published article.

Source Data Figures should be provided as individual PDF files (one file per figure). Authors should endeavor to retain a minimum resolution of 300 dpi or pixels per inch. Please review our instructions for export from Photoshop, Illustrator, and PowerPoint here: https://rupress.org/jcb/pages/submission-guidelines#revised

B. FINAL FILES:

Please upload the following materials to our online submission system. These items are required prior to acceptance. If you have any questions, contact JCB's Managing Editor, Lindsey Hollander (lhollander@rockefeller.edu).

-- An editable version of the final text (.DOC or .DOCX) is needed for copyediting (no PDFs).

-- High-resolution figure and MP4 video files: See our detailed guidelines for preparing your production-ready images,

https://jcb.rupress.org/fig-vid-guidelines.

-- Cover images: If you have any striking images related to this story, we would be happy to consider them for inclusion on the journal cover. Submitted images may also be chosen for highlighting on the journal table of contents or JCB homepage carousel. Images should be uploaded as TIFF or EPS files and must be at least 300 dpi resolution.

It is JCB policy that if requested, original data images must be made available to the editors. Failure to provide original images upon request will result in unavoidable delays in publication. Please ensure that you have access to all original data images prior to final submission.

The license to publish form must be signed before your manuscript can be sent to production. A link to the electronic license to publish form will be sent to the corresponding author only. Please take a moment to check your funder requirements before choosing the appropriate license.

Additionally, JCB encourages authors to submit a short video summary of their work. These videos are intended to convey the main messages of the study to a non-specialist, scientific audience. Think of them as an extended version of your abstract, or a short poster presentation. We encourage first authors to present the results to increase their visibility. The videos will be shared on social media to promote your work. For more detailed guidelines and tips on preparing your video, please visit https://rupress.org/jcb/pages/submission-guidelines#videoSummaries.

Thank you for your attention to these final processing requirements. Please revise and format the manuscript and upload materials within 7 days. If complications arising from measures taken to prevent the spread of COVID-19 will prevent you from meeting this deadline (e.g. if you cannot retrieve necessary files from your laboratory, etc.), please let us know and we can work with you to determine a suitable revision period.

Please contact the journal office with any questions at cellbio@rockefeller.edu.

Thank you for this interesting contribution, we look forward to publishing your paper in Journal of Cell Biology.

Sincerely,

Harald Stenmark
Monitoring Editor
Journal of Cell Biology

Tim Fessenden
Scientific Editor
Journal of Cell Biology

Reviewer #1 (Comments to the Authors (Required)):

In this revision, all of my concerns have been addressed except for one very minor issue. I do not agree with the statement "Overall, we suggest that Gyp7 activity shifts Ypt7 from a primary vacuolar localization to a subset of endosomes" (lines 351-352). Under wild-type conditions, Ypt7 localization is primarily at the vacuole and Gyp7 localization is on endosomes. Only under perturbation conditions (Gyp7 overexpression) does Ypt7 relocalize to endosomes. The overexpression condition does not tell us what the function of normal Gyp7 activity is, as overexpression may cause gain of function. I suggest removing this sentence.

Reviewer #2 (Comments to the Authors (Required)):

I think the authors have addressed all of the most significant technical concerns with the experiments.

I am still on the fence with respect to the "signaling endosome" concept (at least in budding yeast). For example, it remains unclear (to me, at least) whether these entities represent one of a diversified set of distinct endosomal maturation pathways, or instead a transient intermediate on a common maturation pathway. This question does not seem to be resolved.

Hence, I could argue with the conceptual framework. However, I think that there are many useful experiments in this study, and that the conceptual framing is at least plausible enough to serve as a useful working model. Consequently I think that both the results and ideas here will move the field forward, and that the paper should be published without additional delay.

Minor points:
Fig 2 C-E, It might be worth mentioning that the estimated copy number of Zrc1 is significantly higher than that of Gyp7 [http://dx.doi.org/10.1016/j.cels.2017.12.004]. Excess of receptor over ligand-fused target protein is an important precondition for a knock-sideways experiment, and here it seems to be satisfied.

The paper by Generoso et al. (cited in Methods) is not in the Bibliography.

Reviewer #3 (Comments to the Authors (Required)):

My only real concern was a lack of novelty. This concern was apparently not shared by the other two reviewers and the editors, rendering my comment obsolete. I thought that the data were of high quality and the conclusions appeared sound so there are no further objections from my side.

UNIVERSITÄT OSNABRÜCK

Fachbereich
Biologie/Chemie

Abt. Biochemie

PROF. DR. CHRISTIAN UNGERMANN
(HANS-MÜHLENHOFF-STIFTUNGSPROFESSUR)

Barbarastraße 13
49076 Osnabrück
Telefon: +49 541 969 2752
Telefax: +49 541 969 2884

www.uni-osnabrueck.de

Universität Osnabrück · FB 5 · 49076 Osnabrück

To
Andrea Marat
Senior Editor at *JCB*

6th of March, 2024

Dear Andrea, dear Harald,

In response to the reviewers' requests and the editorial instructions, we have adjusted the manuscript. Our corrections are indicated below.

Best,

_____

A. MANUSCRIPT ORGANIZATION AND FORMATTING:

Full guidelines are available on our Instructions for Authors page, http://jcb.rupress.org/submission-guidelines#revised. Submission of a paper that does not conform to JCB guidelines will delay the acceptance of your manuscript.

1) Text limits: Character count for Articles is < 40,000, not including spaces. Count includes abstract, introduction, results, discussion, and acknowledgments. Count does not include title page, figure legends, materials and methods, references, tables, or supplemental legends.

Done

2) Figures limits: Articles may have up to 10 main figures and 5 supplemental figures/tables.
** Please combine supplemental figure panels into corresponding main figure panels, or eliminate supplemental data to reduce total supplemental figures to 5. If appropriate, an additional main figure may also be generated.

Supplemental Figures have been adjusted to 5 in total.

3) Figure formatting: Scale bars must be present on all microscopy images, including

inset magnifications. Molecular weight or nucleic acid size markers must be included on all gel electrophoresis. Please avoid pairing red and green for images and graphs to ensure legibility for color-blind readers. If red and green are paired for images, please ensure that the particular red and green hues used in micrographs are distinctive with any of the colorblind types. If not, please modify colors accordingly or provide separate images of the individual channels.
** Please include scale bars on Figure 9B and S1A.
** Please add molecular weight markers to Fig S7A.

Done

4) Statistical analysis: Error bars on graphic representations of numerical data must be clearly described in the figure legend. The number of independent data points (n) represented in a graph must be indicated in the legend. Statistical methods should be explained in full in the materials and methods. For figures presenting pooled data the statistical measure should be defined in the figure legends. Please also be sure to indicate the statistical tests used in each of your experiments (either in the figure legend itself or in a separate methods section) as well as the parameters of the test (for example, if you ran a t-test, please indicate if it was one- or two-sided, etc.). Also, if you used parametric tests, please indicate if the data distribution was tested for normality (and if so, how). If not, you must state something to the effect that "Data distribution was assumed to be normal but this was not formally tested."

A section has been added.

5) Abstract and title: The abstract should be no longer than 160 words and should communicate the significance of the paper for a general audience. The title should be less than 100 characters including spaces. Make the title concise but accessible to a general readership.
** We recommend changing the title to something slightly shorter: "The GTPase activating protein Gyp7 regulates Rab7/Ypt7 activity on late endosomes"

We agree and adjusted the title accordingly.

6) Materials and methods: Should be comprehensive and not simply reference a previous publication for details on how an experiment was performed. Please provide full descriptions in the text for readers who may not have access to referenced manuscripts. We also provide a report from SciScore and an associate score, which we encourage you to use as a means of evaluating and improving the methods section.
** Please provide full details for in vitro prenylation of Rab GTPases and immune-electron microscopy.

Now included.

7) Please be sure to provide the sequences for all of your primers/oligos and RNAi constructs in the materials and methods. You must also indicate in the methods the

source, species, and catalog numbers (where appropriate) for all of your antibodies. Please also indicate the acquisition and quantification methods for immunoblotting/western blots.

A primer Table is included.

8) Microscope image acquisition: The following information must be provided about the acquisition and processing of images:
a. Make and model of microscope
b. Type, magnification, and numerical aperture of the objective lenses
c. Temperature
d. Imaging medium
e. Fluorochromes
f. Camera make and model
g. Acquisition software
h. Any software used for image processing subsequent to data acquisition. Please include details and types of operations involved (e.g., type of deconvolution, 3D reconstitutions, surface or volume rendering, gamma adjustments, etc.).

All details have been included now.

9) References: There is no limit to the number of references cited in a manuscript. References should be cited parenthetically in the text by author and year of publication. Abbreviate the names of journals according to PubMed.

This has been done.

10) Supplemental materials: There are strict limits on the allowable amount of supplemental data. Articles may have up to 5 supplemental figures. Please also note that tables, like figures, should be provided as individual, editable files. A summary of all supplemental material should appear at the end of the Materials and methods section.

Done.

11) eTOC summary: A ~40-50-word summary that describes the context and significance of the findings for a general readership should be included on the title page. The statement should be written in the present tense and refer to the work in the third person.

Done.

12) Conflict of interest statement: JCB requires inclusion of a statement in the acknowledgements regarding competing financial interests. If no competing financial interests exist, please include the following statement: "The authors declare no competing financial interests." If competing interests are declared, please follow your statement of these competing interests with the following statement: "The authors declare no further competing financial interests."

Done.

13) ORCID IDs: ORCID IDs are unique identifiers allowing researchers to create a record of their various scholarly contributions in a single place. At resubmission of your final files, please provide an ORCID ID for all authors.

Done.

14) A separate author contribution section following the Acknowledgments. All authors should be mentioned and designated by their full names. We encourage use of the CRediT nomenclature.

Done.

15) A data availability statement is required for all research article submissions. The statement should address all data underlying the research presented in the manuscript. Please visit the JCB instructions for authors for guidelines and examples of statements at (https://rupress.org/jcb/pages/editorial-policies#data-availability-statement).

Please note that JCB requires authors to submit Source Data used to generate figures containing gels and Western blots with all revised manuscripts. This Source Data consists of fully uncropped and unprocessed images for each gel/blot displayed in the main and supplemental figures. Since your paper includes cropped gel and/or blot images, please be sure to provide one Source Data file for each figure that contains gels and/or blots along with your revised manuscript files. File names for Source Data figures should be alphanumeric without any spaces or special characters (i.e., SourceDataF#, where F# refers to the associated main figure number or SourceDataFS# for those associated with Supplementary figures). The lanes of the gels/blots should be labeled as they are in the associated figure, the place where cropping was applied should be marked (with a box), and molecular weight/size standards should be labeled wherever possible. Source Data files will be directly linked to specific figures in the published article.

Source Data Figures should be provided as individual PDF files (one file per figure). Authors should endeavor to retain a minimum resolution of 300 dpi or pixels per inch. Please review our instructions for export from Photoshop, Illustrator, and PowerPoint here: https://rupress.org/jcb/pages/submission-guidelines#revised

A statement has been added accordingly.

B. FINAL FILES:

Please upload the following materials to our online submission system. These items are required prior to acceptance. If you have any questions, contact JCB's Managing Editor, Lindsey Hollander (lhollander@rockefeller.edu).

-- An editable version of the final text (.DOC or .DOCX) is needed for copyediting (no PDFs).

-- High-resolution figure and MP4 video files: See our detailed guidelines for preparing your production-ready images, https://jcb.rupress.org/fig-vid-guidelines.

-- Cover images: If you have any striking images related to this story, we would be happy to consider them for inclusion on the journal cover. Submitted images may also be chosen for highlighting on the journal table of contents or JCB homepage carousel. Images should be uploaded as TIFF or EPS files and must be at least 300 dpi resolution.

It is JCB policy that if requested, original data images must be made available to the editors. Failure to provide original images upon request will result in unavoidable delays in publication. Please ensure that you have access to all original data images prior to final submission.

The license to publish form must be signed before your manuscript can be sent to production. A link to the electronic license to publish form will be sent to the corresponding author only. Please take a moment to check your funder requirements before choosing the appropriate license.

Additionally, JCB encourages authors to submit a short video summary of their work. These videos are intended to convey the main messages of the study to a non-specialist, scientific audience. Think of them as an extended version of your abstract, or a short poster presentation. We encourage first authors to present the results to increase their visibility. The videos will be shared on social media to promote your work. For more detailed guidelines and tips on preparing your video, please visit https://rupress.org/jcb/pages/submission-guidelines#videoSummaries.

Thank you for your attention to these final processing requirements. Please revise and format the manuscript and upload materials within 7 days. If complications arising from measures taken to prevent the spread of COVID-19 will prevent you from meeting this deadline (e.g. if you cannot retrieve necessary files from your laboratory, etc.), please let us know and we can work with you to determine a suitable revision period.

Please contact the journal office with any questions at cellbio@rockefeller.edu.

Thank you for this interesting contribution, we look forward to publishing your paper in Journal of Cell Biology.

Sincerely,

Harald Stenmark
Monitoring Editor
Journal of Cell Biology

Tim Fessenden
Scientific Editor
Journal of Cell Biology

Reviewer #1 (Comments to the Authors (Required)):

In this revision, all of my concerns have been addressed except for one very minor issue. I do not agree with the statement "Overall, we suggest that Gyp7 activity shifts Ypt7 from a primary vacuolar localization to a subset of endosomes" (lines 351-352). Under wild-type conditions, Ypt7 localization is primarily at the vacuole and Gyp7 localization is on endosomes. Only under perturbation conditions (Gyp7 overexpression) does Ypt7 relocalize to endosomes. The overexpression condition does not tell us what the function of normal Gyp7 activity is, as overexpression may cause gain of function. I suggest removing this sentence.

Thank you. We removed the sentence as requested.

Reviewer #2 (Comments to the Authors (Required)):

I think the authors have addressed all of the most significant technical concerns with the experiments.

I am still on the fence with respect to the "signaling endosome" concept (at least in budding yeast). For example, it remains unclear (to me, at least) whether these entities represent one of a diversified set of distinct endosomal maturation pathways, or instead a transient intermediate on a common maturation pathway. This question does not seem to be resolved.

Hence, I could argue with the conceptual framework. However, I think that there are many useful experiments in this study, and that the conceptual framing is at least plausible enough to serve as a useful working model. Consequently I think that both the results and ideas here will move the field forward, and that the paper should be published without additional delay.

Thank you for the kind feedback.

Minor points:
Fig 2 C-E, It might be worth mentioning that the estimated copy number of Zrc1 is significantly higher than that of Gyp7 [http://dx.doi.org/10.1016/j.cels.2017.12.004]. Excess of receptor over ligand-fused target protein is an important precondition for a knock-sideways experiment, and here it seems to be satisfied.

Thank you, the reference was included and a statement was added to the text.

The paper by Generoso et al. (cited in Methods) is not in the Bibliography.

Now added.

Reviewer #3 (Comments to the Authors (Required)):

My only real concern was a lack of novelty. This concern was apparently not shared by the other two reviewers and the editors, rendering my comment obsolete. I thought that the data were of high quality and the conclusions appeared sound so there are no further objections from my side.

We appreciate that the reviewer acknowledges our efforts and agrees with the publication.